**Biogeosciences**

Open Access

# Sea–air CO$_2$ fluxes in the Southern Ocean for the period 1990–2009

**A. Lenton**[1], **B. Tilbrook**[1,2], **R. M. Law**[3], **D. Bakker**[4], **S. C. Doney**[5], **N. Gruber**[6], **M. Ishii**[7], **M. Hoppema**[8],
**N. S. Lovenduski**[9], **R. J. Matear**[10], **B. I. McNeil**[11], **N. Metzl**[12], **S. E. Mikaloff Fletcher**[13], **P. M. S. Monteiro**[14],
**C. Rödenbeck**[15], **C. Sweeney**[16], and **T. Takahashi**[17]

[1]Centre for Australian Weather and Climate Research, CSIRO Marine and Atmospheric Research, Hobart, Tasmania, Australia
[2]Antarctic Climate Ecosystems Co-operative Research Centre, Hobart, Tasmania, Australia
[3]Centre for Australian Weather and Climate Research, CSIRO Marine and Atmospheric Research, Aspendale, Victoria, Australia
[4]School of Environmental Sciences, University of East Anglia Research Park, Norwich NR4 7TJ, UK
[5]Marine Chemistry and Geochemistry Dept., Woods Hole Oceanographic Institution, Woods Hole, MA 02543, USA
[6]Institute of Biogeochemistry and Pollutant Dynamics and Center for Climate Systems Modeling, ETH Zurich, Zurich, Switzerland
[7]Meteorological Research Institute, Tsukuba 305-0031, Japan
[8]Alfred Wegener Institute, Bremerhaven, Germany
[9]Department of Atmospheric and Oceanic Sciences, Institute of Arctic and Alpine Research, University of Colorado, Boulder, CO 80309, USA
[10]Centre for Australian Weather and Climate Research, CSIRO Marine and Atmospheric Research, Hobart, Tasmania, Australia
[11]Climate Change Research Centre, University of New South Wales, Sydney, Australia
[12]Laboratoire d'Océanographie et du Climat, LOCEAN/IPSL, CNRS, Université Pierre et Marie Curie, Paris, France
[13]National Institute of Water and Atmospheric Research, Wellington 6021, New Zealand
[14]Department of Oceanography, University of Cape Town, Rondebosch 7700, South Africa and Ocean Systems & Climate Group, CSIR, Stellenbosch, South Africa
[15]Max-Planck-Institute for Biogeochemistry, 07745 Jena, Germany
[16]Cooperative Institute for Research in Environmental Science, University of Colorado, Boulder, CO 80305, USA
[17]Lamont-Doherty Earth Observatory of Columbia University, Palisades, New York, USA

*Correspondence to:* A. Lenton (andrew.lenton@csiro.au)

**Abstract.** The Southern Ocean (44–75° S) plays a critical role in the global carbon cycle, yet remains one of the most poorly sampled ocean regions. Different approaches have been used to estimate sea–air CO$_2$ fluxes in this region: synthesis of surface ocean observations, ocean biogeochemical models, and atmospheric and ocean inversions. As part of the RECCAP (REgional Carbon Cycle Assessment and Processes) project, we combine these different approaches to quantify and assess the magnitude and variability in Southern Ocean sea–air CO$_2$ fluxes between 1990–2009. Using all models and inversions (26), the integrated median annual sea–air CO$_2$ flux of $-0.42 \pm 0.07$ Pg C yr$^{-1}$ for the 44–75° S region, is consistent with the $-0.27 \pm 0.13$ Pg C yr$^{-1}$ calculated using surface observations. The circumpolar region south of 58° S has a small net annual flux (model and inversion median: $-0.04 \pm 0.07$ Pg C yr$^{-1}$ and observations: $+0.04 \pm 0.02$ Pg C yr$^{-1}$), with most of the net annual flux located in the 44 to 58° S circumpolar band (model and inversion median: $-0.36 \pm 0.09$ Pg C yr$^{-1}$ and observations: $-0.35 \pm 0.09$ Pg C yr$^{-1}$). Seasonally, in the 44–58° S region, the median of 5 ocean biogeochemical models captures the observed sea–air CO$_2$ flux seasonal cycle, while the median

of 11 atmospheric inversions shows little seasonal change in the net flux. South of 58° S, neither atmospheric inversions nor ocean biogeochemical models reproduce the phase and amplitude of the observed seasonal sea–air $CO_2$ flux, particularly in the Austral Winter. Importantly, no individual atmospheric inversion or ocean biogeochemical model is capable of reproducing both the observed annual mean uptake and the observed seasonal cycle. This raises concerns about projecting future changes in Southern Ocean $CO_2$ fluxes. The median interannual variability from atmospheric inversions and ocean biogeochemical models is substantial in the Southern Ocean; up to 25 % of the annual mean flux, with 25 % of this interannual variability attributed to the region south of 58° S. Resolving long-term trends is difficult due to the large interannual variability and short time frame (1990–2009) of this study; this is particularly evident from the large spread in trends from inversions and ocean biogeochemical models. Nevertheless, in the period 1990–2009 ocean biogeochemical models do show increasing oceanic uptake consistent with the expected increase of $-0.05\,\mathrm{Pg\,C\,yr^{-1}\,decade^{-1}}$. In contrast, atmospheric inversions suggest little change in the strength of the $CO_2$ sink broadly consistent with the results of Le Quéré et al. (2007).

## 1 Introduction

Over recent decades, the ocean has taken up about 25 % of the annual anthropogenic $CO_2$ emissions to the atmosphere from fossil fuel burning, cement production, and land-use change (Le Quéré et al., 2009), slowing the growth of atmospheric $CO_2$ and therefore the rate of climate change. The Southern Ocean, defined here as the oceanic region south of 44° S, is a key region in the global uptake of anthropogenic $CO_2$ (Caldeira and Duffy, 2000; Mikaloff Fletcher et al., 2006). This region accounts for about one-third of the total global ocean uptake of anthropogenic $CO_2$ (c.a. $0.7\,\mathrm{Pg\,C\,yr^{-1}}$), even though it covers less than 20 % of the global ocean surface area (Mikaloff Fletcher et al., 2006; Gruber et al., 2009). This uptake flux of anthropogenic $CO_2$ is partially compensated by the degassing of natural $CO_2$ (Mikaloff Fletcher et al., 2007), so that the contemporary uptake is smaller than that of anthropogenic $CO_2$ alone (Takahashi et al., 2009). Projections suggest that the region will continue to be an important sink of atmospheric $CO_2$, although the efficiency of the sink may decrease (Roy et al., 2011). Despite its importance, the Southern Ocean remains one of the most poorly sampled ocean regions with respect to carbon dioxide (Monteiro et al., 2010; Fig. 2).

The Southern Ocean is dominated by the eastward flowing Antarctic Circumpolar Current (ACC). A northward Ekman transport at the surface of the ACC creates a divergence driven upwelling of carbon-rich water near the southern boundary of the ACC. The upwelling of mid-
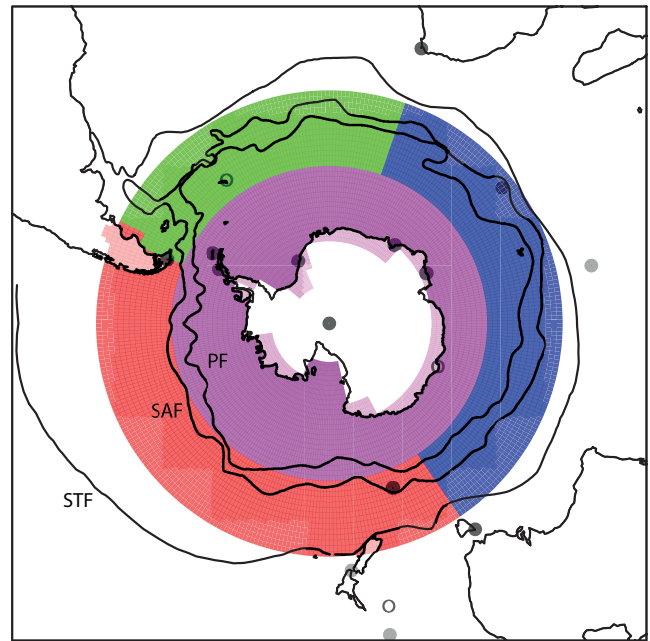


**Fig. 1.** Subregions of the Southern Ocean (44 to 75° S) used in this paper are the circular region 44–58° S (green, red and blue combined) and the major ocean basins (Pacific, Indian and Atlantic) in this band, and the circumpolar region from 58–75° S (purple). Overlain is the network of atmospheric observations of $CO_2$. The colour of the dot indicates how many inversions used data from that location (dark grey: all or almost all inversions, light grey: around half the inversions, white: one or two inversions). We note that the temporal period over which the data was collected is not the same in all the stations. Overlain on these figures, from north to south are the mean positions of the major fronts subtropical front (STF), Subantarctic front (SAF) and the Polar Front (PF) following Orsi et al. (1995).

depth (2–2.5 km) water creates a unique connection between the deep ocean and the atmosphere, while the subduction of mode and intermediate waters further north links the Southern Ocean with waters that resurface at low latitudes (Sarmiento et al., 2004). The connections between the surface and ocean interior make the Southern Ocean an important region for controlling ocean–atmosphere carbon exchange and are a major influence in setting atmospheric $CO_2$ levels (Sallee et al., 2012).

The Southern Ocean is comprised of a series of key zones in terms of carbon dynamics (Fig. 1). These zones from north to south are (i) the Subantarctic zone (SAZ) between the subtropical front (STF) and the Subantarctic front (SAF), nominally 40–50° S; (ii) the polar frontal zone (PFZ), between the SAF and the polar front (PF), nominally 50–55° S; (iii) the Antarctic zone (AZ) between the PF and the Antarctic coastline, taking in the marginal seas and the seasonal ice zone (SIZ).
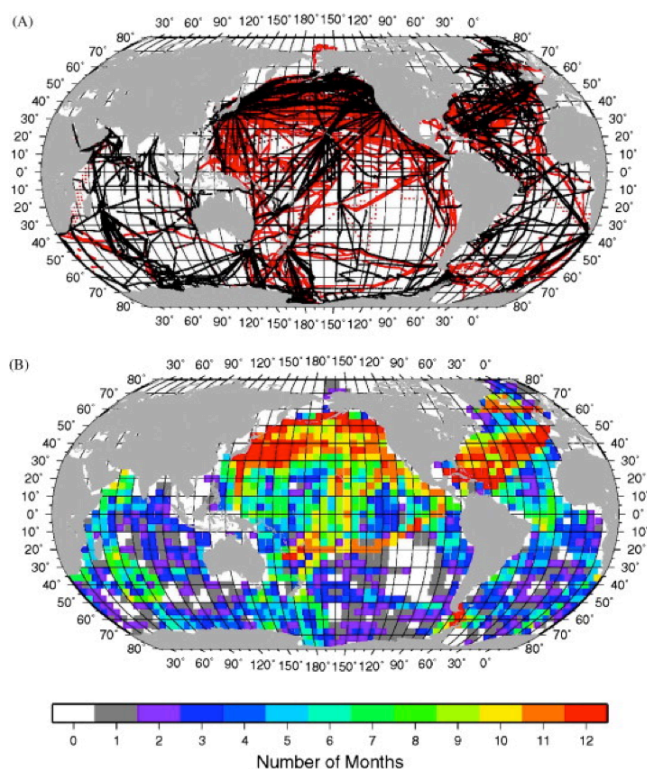
**Fig. 2.** The upper figure shows the location of observations of oceanic $p$CO$_2$. Black dots indicate the database ($\sim 1$ million $p$CO$_2$ measurement) used for Takahashi et al. (2002); and red dots indicate an additional $\sim 3$ million data points used for Takahashi et al. (2009). The lower panel shows the number of months of the year for which observations exist. This data is the basis of the observational data used in this study (reproduced from Takahashi et al., 2009).

The available observations indicate that the seasonal cycle is the dominant mode of variability in the surface partial pressure of CO$_2$ ($p$CO$_2$) and the sea–air exchange for the Southern Ocean (Lenton et al., 2006; Thomalla et al., 2011). Oceanic uptake of CO$_2$ from the atmosphere corresponds to a negative net sea–air CO$_2$ flux, and an oceanic source of CO$_2$ to the atmosphere has a positive net sea–air flux. Increased biological production in summer tends to reduce the $p$CO$_2$ and increase the net ocean uptake of CO$_2$. Lower biological production and deeper mixing that entrains more CO$_2$-rich water into the mixed layer has the opposite effect in winter. Seasonal temperature changes offset the biological and mixing related effects on surface $p$CO$_2$ and act to mute the variability in seasonal sea–air fluxes (e.g. Takahashi et al., 2002 and Takahashi et al., 2009). While the biological and physical mechanisms driving this seasonal variability are relatively well known, their magnitude and phase remain poorly constrained (Metzl et al., 2006; Lenton et al., 2006).

In the austral summer the PFZ and SAZ act as strong sinks of atmospheric CO$_2$ due to enhanced biological production (Metzl et al., 1999; Takahashi et al., 2009, 2012). In the Aus-

tral Winter, the net uptake of CO$_2$ in the PFZ and SAZ is reduced relative to summer, and in some areas a net outgassing occurs as a result of deep winter mixing entraining carbon-rich waters from the ocean interior into the surface mixed layer. When integrated annually, these regions act as a strong net sink of atmospheric CO$_2$, with the largest uptake occurring in the SAZ and decreasing southward (Metzl et al., 1999, 2006; McNeil et al., 2007; Takahashi et al., 2012).

The AZ to the south of the PFZ contains a permanently ice free region in the north that transitions poleward to waters covered seasonally by sea ice with some permanently ice-covered waters at high latitudes. The seasonal ice covered region in the south portion of the AZ acts as a sink of atmospheric CO$_2$ in summer as sea-ice retreats and increased stratification of the upper water column and greater light availability leads to an increase in the biological drawdown of carbon (Ishii et al., 1998; Bakker et al., 2008). Sea-ice cover inhibits sea–air gas exchange in winter, although there is considerable uncertainty as to how the ice cover impacts sea–air fluxes at high latitudes in winter months (e.g. Rysgaard et al., 2011 and Loose and Schlosser, 2011). In the permanently ice free region of the AZ, $p$CO$_2$ tends to be lower than the atmosphere in summer owing to net biological production (Ishii et al., 2002; Metzl et al., 2006; Sokolov, 2008) and higher than the atmosphere in winter due to deep winter mixing. Integrated annually, the observations suggest the AZ acts as a neutral or weak source of atmospheric CO$_2$ (Takahashi et al., 2009).

In recent decades, a strengthening of the Southern Annular Mode (SAM), driven by increasing greenhouse gases and stratospheric ozone depletion, has resulted in a southward shift and intensification of the zonal winds, and increases in heat and freshwater fluxes over the Southern Ocean (Thompson and Solomon, 2002). During this period, oceanic $p$CO$_2$ growth rates based on limited observations (Metzl, 2009; Takahashi et al., 2009) and some atmospheric inversions and ocean biogeochemical models (Le Quéré et al., 2007) have suggested a decrease in the efficiency of the Southern Ocean CO$_2$ sink in response to these physical changes. The strengthening SAM is believed to increase the upwelling of carbon-rich deep water that results in a decrease in the net ocean carbon uptake due to a change in the sea–air gradient in $p$CO$_2$ (Le Quéré et al., 2007; Lovenduski et al., 2007; Lenton and Matear, 2007; Lenton et al., 2009). The corresponding changes in primary productivity are small relative to the response of ocean dynamics (Lenton et al., 2009). Furthermore, this change may have enhanced the outgassing of natural CO$_2$ and had only a small effect on the uptake of anthropogenic CO$_2$ (Lovenduski et al., 2008; Matear and Lenton, 2008). Evidence for a reduced efficiency of the Southern Ocean sink is not supported by all atmospheric inversions (e.g. Law et al., 2008). Analyses of long-running atmospheric CO$_2$ time series in the Southern Hemisphere and model simulations suggest that it may not be possible to robustly detect a slowdown in the Southern Ocean sink

from atmospheric CO$_2$ measurements at present (Stephens et al., 2013). Furthermore, ocean observations also suggest the changes in the sink efficiency may not be zonally uniform for the Southern Ocean (Lenton et al., 2012).

Different approaches have been used to estimate the total sea–air CO$_2$ fluxes (i.e. the anthropogenic + natural (or pre-industrial)) in the Southern Ocean, including (i) synthesis of surface ocean $p$CO$_2$ observations with empirical gas exchange parameterizations, and using interpolation schemes applied to ocean $p$CO$_2$ observations to address sparse data coverage; (ii) prognostic ocean biogeochemical models based on physical ocean general circulation models coupled with biogeochemical models; (iii) atmospheric inversion studies, based on the inversion of atmospheric CO$_2$ data; and (iv) ocean inversion models, based on ocean interior measurements and ocean model simulations. Historically, these modelling approaches have produced significantly different annual mean estimates of Southern Ocean sea–air fluxes of carbon (e.g. Roy et al., 2003). A more recent study suggests there is growing agreement in the magnitude of the annual flux for the region (Gruber et al., 2009), although substantial differences remain with regard to the meridional distribution.

In this study we compare the total sea–air CO$_2$ fluxes in the Southern Ocean derived from observations, atmospheric and ocean inverse calculations, and ocean biogeochemical models for the period 1990–2009. The oceanic exchange of CO$_2$ with the atmosphere through sea–air gas flux is driven by the difference in $\Delta p$CO$_2$ between the ocean and the overlying atmosphere and is a function of wind-speed.

The goals of this work are to (i) quantify the annual sea–air flux of CO$_2$; (ii) assess the sea–air flux and its relationship with the annual mean uptake; (iii) quantify the magnitude of interannual variability in the Southern Ocean and investigate the long-term trends of ocean carbon uptake. This work is part of the REgional Carbon Cycle Assessment and Processes project (RECCAP; Canadell et al., 2011) led by the Global Carbon Project, and this paper is part of a special volume of papers assessing the variability in the global carbon cycle over the period 1990–2009.

## 2 Methods

### 2.1 Datasets

The regional sea–air CO$_2$ fluxes described below use REC-CAP "Tier 1" global CO$_2$ flux products (Canadell et al., 2011). These products include datasets of CO$_2$ fluxes from observations, ocean biogeochemical models, atmospheric and ocean inversions.

### 2.1.1 Observations

The Southern Ocean remains one of the most poorly sampled ocean regions with respect to carbon (Fig. 2), with some regions in the eastern South Pacific yet to be sampled. To account for this paucity of sampling, Takahashi et al. (2009) compiled more than 3 million measurements of oceanic $p$CO$_2$ globally, and corrected these to the reference of the year 2000. These values were averaged onto a global grid, and two dimensional advection-diffusion equations were used to interpolate spatially for each month (Takahashi et al., 1997). Wanninkhof et al. (2013) used the Takahashi gridded data and Calibrated Multi-Platform Winds (CCMP; Atlas et al., 2011) to generate a monthly 1° × 1° climatology of net sea–air CO$_2$ fluxes for RECCAP. In our subsequent analysis and comparison with different models and inversions, we define observations as this climatology.

The steep meridional gradients in physical, chemical and biological properties of the Southern Ocean, as well as the patchiness of biological activities, means that the observed $p$CO$_2$ values vary over a wide range in space and time. This combined with errors associated with sparse data coverage, wind speed measurements and gas transfer coefficients (for more discussion see Wanninkhof et al., 2013 and Sweeney et al., 2007) mean that the observationally derived fluxes contain large uncertainties. Therefore, we conservatively estimated an uncertainty on all sea–air CO$_2$ flux observations of ±50 %, consistent with Gruber et al. (2009) and Schuster et al. (2013). There is insufficient observational data to assess the longer-term (interannual to decadal) variability for the entire Southern Ocean, and comparisons of model simulations and observed fluxes are limited in the following sections to the annual and seasonal variability of the total (anthropogenic and preindustrial) net sea–air CO$_2$ fluxes.

### 2.1.2 Ocean biogeochemical models

The simulated sea–air CO$_2$ fluxes come from five ocean general circulation models coupled to ocean biogeochemical models (Table 1). These models represent the physical, chemical and biological processes governing the marine carbon cycle and the exchange of CO$_2$ with the atmosphere. All of these are z-coordinate models of coarse resolution that do not resolve or permit mesoscale eddies. The simulations were driven with observed reanalysis products for atmospheric boundary conditions over the period 1990–2009. All of these models have been integrated from the pre-industrial to present day with the same atmospheric CO$_2$ history. The physical models vary in many aspects such as the details of physical forcing, sub-grid scale parameterizations, and experimental configurations that are detailed in the reference for each model in Table 1. In addition, the models incorporate different biogeochemical modules, e.g. none use the phytoplankton growth model of Geider et al. (2007), which can substantially influence the simulated fields of surface CO$_2$.

**Table 1.** Ocean biogeochemical models used this the study, their respective surface areas between 44° S and 75° S, the periods over which the data was evaluated, and the reference to each model.

| Model Name | Period | Area (km$^2$) | Forcing | Gas Exchange | Ecosystem structure | Limiting Nutrient | Sea ice | Reference |
|---|---|---|---|---|---|---|---|---|
| CSIRO | 1990–2009 | $6.154 \times 10^7$ | NCEP–R1 | Wanninkhof (1992) | none (nutrient-restoring model) | P | No | Matear and Lenton (2008) |
| CCSM-BEC | 1990–2009 | $6.102 \times 10^7$ | NCEP–R1 | Wanninkhof (1992) | 4 phytoplankton + 1 zooplankton | N, P, Si, Fe | Yes | Thomas et al. (2008) |
| NEMO-PlankTOM5 | 1990–2009 | $6.217 \times 10^7$ | NCEP–R1 | Wanninkhof (1992) | 2 phytoplankton + 2 zooplankton | N, P, Si, Fe | Yes | Le Quéré et al. (2007) |
| NEMO-PISCES | 1990–2009 | $6.102 \times 10^7$ | NCEP–R1 | Wanninkhof (1992) | 3 phytoplankton + 2 zooplankton | N, P, Si, Fe | Yes | Aumont and Bopp (2006) |
| CCSM-ETH | 1990–2007 | $6.140 \times 10^7$ | CORE–2 | Wanninkhof (1992)* | 4 phytoplankton + 1 zooplankton | N, P, Si, Fe | Yes | Graven et al. (2012) |

* With a coefficient of $0.24 \, \text{cm} \, \text{h}^{-1} \, \text{s}^2 \, \text{m}^{-2}$.

### 2.1.3 Atmospheric inversions

Inversions of atmospheric CO$_2$ measurements use an atmospheric transport model and an optimization technique to determine carbon fluxes that best fit the atmospheric measurements. In most cases, a first guess or a priori flux based on independent datasets or models is also used to further constrain the flux estimates. Here we use the same set of atmospheric CO$_2$ inversions as described in Peylin et al. (2013). The inversions (Table 2) vary in many aspects, such as the atmospheric transport model, sea–air CO$_2$ flux resolution, solution method, a priori estimates and the atmospheric CO$_2$ datasets.

In this study, we consider inversions that solve for carbon fluxes at a variety of different spatial resolutions, dividing the Southern Ocean region into between 1 and 14 regions or, in some cases, solving at the resolution of the transport model used in the inversion. In cases where inversions solved for regions that cross the 44° S boundary used in this analysis, a proportion of the estimated flux is used, based on any assumptions about the flux distribution within a region. For the inversions solving at grid-cell resolution, those methods use a correlation length scale to ensure relatively smoothly varying fluxes.

Figure 1 shows atmospheric-CO$_2$ measurement sites south of 30° S that were used by the inversions. Most sites were used by all or almost all the inversions, while Amsterdam Island (78° E, 37° S), Baring Head (175° E, 41° S) and ship data (169° E, 30° S) were used by only about half the inversions (grey circles). There are three sites that are only used by one or two inversions. Many inversions use monthly mean atmospheric concentrations derived from the pseudo-weekly filtered data from the GLOBALVIEW-CO$_2$ data product (e.g. GLOBALVIEW-CO$_2$, 2011 and earlier annual releases). Four inversions use "raw" data (i.e. the inversions include flask observations at the appropriate sampling time) or hourly observations if these are available, though generally with some selection based on time of day. All but three

inversions account for interannual variations in atmospheric transport.

An important consideration when interpreting the inverse estimates is to understand the influence of any prior information used in the inversion. For example, in almost all the inversions considered here, ocean CO$_2$ fluxes derived from $p$CO$_2$ measurements (e.g. Takahashi et al., 1999 or Takahashi et al., 2009) were used to constrain the sea–air fluxes, so that the inversion is actually estimating sea–air fluxes that are deviations from the prior Takahashi-based estimates. Depending on the spatial resolution of the inversion and the additional constraints that have been incorporated into the inversion, the basin-scale flux information may be strongly dependent on the prior information rather than new independent information derived from the local atmospheric CO$_2$ measurements.

### 2.1.4 Ocean inversions

In this paper we use ten ocean inverse model simulations presented in Gruber et al. (2009) and the mean value across these simulations calculated from three periods: 1995, 2000 and 2005. As this technique only solves for an annual mean state, i.e. does not resolve seasonality or interannual variability, these simulations are only used to assess the annual uptake. The specific details on methods and models used in these ocean inversions are detailed in Mikaloff Fletcher et al. (2006, 2007) and Gruber et al. (2009).

Gruber et al. (2009) used a suite of ten different ocean biogeochemical models to estimate the uncertainty of the flux estimates due to model transport, and weighted these models using a skill score based on each model's ability to accurately represent pre-bomb radiocarbon and CFCs when calculating the mean and standard deviations of the models. However, here we have chosen to give all of the models equal weight in order to be consistent with our analysis of ocean models and atmospheric inversions, where no weighting scheme was used.

**Table 2.** Atmospheric inverse models and periods over which data was evaluated in this study, the number of sites south of 30° S, model resolution and the reference to each model.

| Model Name | Period[a] | Sites used 30–90° S | Flux res. in S Ocn[b] | Reference |
|---|---|---|---|---|
| LSCE_an_v2.1 | 1996–2004 | 11 | 3.75° × 2.5° | Piao et al. (2009) |
| LSCE_var_v1.0 | 1990–2008 | 14 | 3.75° × 2.5° | Chevallier et al. (2010) |
| C13_CCAM_law | 1992–2008 | 14 | 14 | Rayner et al. (2008) |
| C13_MATCH_rayner | 1992–2008 | 14 | 6 | Rayner et al. (2008) |
| CTRACKER_US[c] | 2001–2008 | 10 | 4 | Peters et al. (2007) |
| CTRACKER_EU | 2001–2008 | 7 | 4 | Peters et al. (2010) |
| JENA_s96_v3.3 | 1996–2008 | 13 | 5° × 3.75° | Rödenbeck (2005) |
| TRCOM_mean_9008 | 1990–2008 | 12 | 1 | Baker et al. (2006) |
| RIGC_patra | 1990–2008 | 12 | 2 | Patra et al. (2005) |
| JMA_2010 | 1990–2008 | 15 | 1 | Maki et al. (2010) |
| NICAM_niwa_woaia | 1990–2007 | 15 | 1 | Niwa et al. (2012)[d] |

[a] Period used for analysis. Inversions may have been run for a longer time.
[b] Longitude × latitude if inversion solves for each grid cell, otherwise number of ocean regions south of 44° S.
[c] CT2009 release.
[d] Inversion method as this reference, except CONTRAIL aircraft CO$_2$ data not used for RECCAP inversion.

The skill score weighting has a relatively minor influence on fluxes over most of the ocean. However, in the Southern Ocean, the skill score weighting leads to a smaller net uptake of CO$_2$ by the Southern Ocean and a different distribution of the uptake between regions. This is because some models used in the ocean inversion tend to overestimate CFC concentrations in the Southern Ocean relative to observations, and also estimate substantially higher anthropogenic CO$_2$ uptake in the inversion compared with other contributing models (Mikaloff Fletcher et al., 2006). The skill score-weighting scheme reduces the impact of these models on the weighted mean and therefore leads to a smaller estimated sink.

## 2.2 Study region

Following RECCAP protocols and its regional definitions, we use the latitudinal boundaries of 44–58° S and 58–75° S to define two broad Southern Ocean subdomains (Mikaloff Fletcher et al., 2006). The 44–58° S circumpolar band includes a large part of the SAZ and the PFZ, while the southern region includes the AZ. The region 44–58° S is further split into the three major ocean basins: Indian, Pacific and Atlantic (Fig. 1; Table 3). All together we consider 6 regions in the Southern Ocean (Table 3): the five outlined above and one region comprising the total Southern Ocean south of 44° S.

## 2.3 Calculation and assessment of sea–air CO$_2$ fluxes

The sea–air CO$_2$ fluxes for ocean models and inversions were calculated as a median and the variability as a median absolute deviation (MAD; Gauss, 1816), consistent with Schuster et al. (2013). The MAD is the value where one half of all values are closer to the median than the MAD, and is a useful statistic for excluding outliers in datasets. The calculation of the annual uptake and seasonal variability of sea–air CO$_2$

fluxes from atmospheric inversions and ocean biogeochemical models used data from all of the models and inversions listed in Tables 1 and 2. The seasonality in the sea–air CO$_2$ flux calculated from the individual models was compared to net flux estimates from the surface ocean CO$_2$ climatology for the year 2000 using 2-quadrant Taylor diagrams (Taylor, 2001). This allows both the phase and magnitude of the seasonal cycle for each model to be assessed individually along with the annual mean value. Finally, in the calculation of trends we only used model simulations in which 10 or more years of output was available and assumed the trends were linear following Le Quéré et al. (2007). The sea–air CO$_2$ flux into the ocean is defined as negative, consistent with RECCAP protocols.

## 3 Results and discussion

The modelled and observational based sea–air fluxes of CO$_2$ for the Southern Ocean are evaluated at three scales of variability: (i) annual, (ii) seasonal, and, (iii) interannual for the period 1990–2009.

## 3.1 Annual uptake For 1990 to 2009

The median annual sea–air CO$_2$ flux between 1990 and 2009 is first considered for the entire Southern Ocean (44–75° S) for all available models. Two subdomains are then considered, notably the region 44–58° S that covers the parts of the SAZ and the PFZ, and the region south of 58° S that includes the marginal seas, sea-ice zone and open water regions of the AZ (Fig. 1).

**Table 3.** The annual CO$_2$ uptake (negative into the ocean) from observations (with assumed 50 % uncertainty) and multi-model median uptake (negative into the ocean) and median absolute deviation (MAD) from ocean biogeochemical models, atmospheric and ocean inversions, and all of the models. A, I, P refer to the Atlantic, Indian and Pacific Sectors of the Southern Ocean. All units are Pg C yr$^{-1}$.

| | Area (km$^2$)* | Obs | OBGC models | Atm inversions | Ocean inversions | All models ($n = 26$) |
|---|---|---|---|---|---|---|
| 44–75° S | $6.201 \times 10^7$ | $-0.27 \pm 0.13$ | $-0.43 \pm 0.38$ | $-0.37 \pm 0.13$ | $-0.42 \pm 0.03$ | $-0.42 \pm 0.07$ |
| 44–58° S | $3.837 \times 10^7$ | $-0.32 \pm 0.16$ | $-0.26 \pm 0.20$ | $-0.38 \pm 0.1$ | $-0.35 \pm 0.02$ | $-0.35 \pm 0.09$ |
| A: 44–58° S | $9.237 \times 10^6$ | $-0.09 \pm 0.05$ | $-0.06 \pm 0.04$ | $-0.13 \pm 0.07$ | $-0.14 \pm 0.02$ | $-0.13 \pm 0.04$ |
| I: 44–58° S | $1.304 \times 10^7$ | $-0.1 \pm 0.05$ | $-0.04 \pm 0.12$ | $-0.07 \pm 0.04$ | $-0.12 \pm 0.01$ | $-0.11 \pm 0.03$ |
| P: 44–58° S | $1.610 \times 10^7$ | $-0.13 \pm 0.06$ | $-0.12 \pm 0.08$ | $-0.15 \pm 0.06$ | $-0.11 \pm 0.01$ | $-0.11 \pm 0.04$ |
| 58–75° S | $2.364 \times 10^7$ | $0.04 \pm 0.02$ | $-0.04 \pm 0.09$ | $0.03 \pm 0.03$ | $-0.07 \pm 0.01$ | $-0.04 \pm 0.07$ |

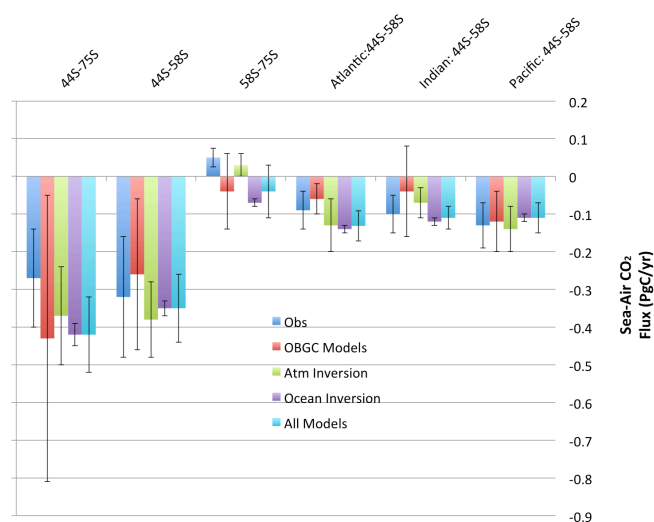* Denotes surface area from observed climatology of Wanninkhof (2012).



**Fig. 3.** Annual median uptake from observations and the median of ocean biogeochemical models, atmospheric inversions and ocean inversions (Pg C yr$^{-1}$). The error bars for each model represent the median absolute deviation (MAD). Negative values represent fluxes into the ocean.

### 3.1.1 Total Southern Ocean 44–75° S

The median annual sea–air CO$_2$ fluxes calculated from observations, models and inversions vary between $-0.27$ and $-0.43$ Pg C yr$^{-1}$ for the entire Southern Ocean region (Table 3 and Fig. 3). The flux estimates from ocean inversions and ocean biogeochemical models, although not significantly different from the other estimates, tend to indicate a stronger uptake. This is consistent with the results of Gruber et al. (2009) who used a subset of the ocean and atmospheric inversions considered here. The agreement in the sea–air flux estimates based on the different approaches is a significant improvement in recent years over previously published studies (e.g. Roy et al., 2003).

The northern boundary of the Southern Ocean is set at 44° S to conform to RECCAP protocols. This excludes some of the SAZ region, which extends to the subtropical front

(STF) at about 40° S in some basins (Fig. 1). The inclusion of the northern part of the SAZ would increase the Southern Ocean CO$_2$ uptake in the global carbon cycle. For example, the annual net uptake from observations nearly doubles from $-0.27 \pm 0.13$ Pg C yr$^{-1}$ to $-0.47 \pm 0.24$ Pg C yr$^{-1}$, when the boundary is shifted from 44 to 40° S.

The largest median absolute deviation (MAD) in the annual sea–air flux is for ocean biogeochemical models (Table 3, Fig. 3). However, the small number of ocean biogeochemical models (5) compared to atmospheric inversions (11) can result in greater MAD values for the ocean models.

The spatial plots of the annual mean uptake for 1990–2009 (Fig. 4) show that all the ocean models simulate a negative sea–air flux or uptake equatorward of 50° S. The CCSM-BEC, CCSM-ETH and CSIRO models have similar patterns of sea–air fluxes as the values derived from observations with areas of CO$_2$ flux to the atmosphere at high latitudes (poleward of 50° S) and areas of CO$_2$ flux into the ocean to the north of the Subantarctic front at about 50° S; however, the fluxes to the atmosphere from these models tend to be greater than the values from observations. The CSIRO model also simulates a region of uptake in the eastern Pacific that is not apparent in the observations, although this region has few measurements to constrain the observational based estimates (Fig. 2). The NEMO-Plankton5 and NEMO-PISCES models simulate larger CO$_2$ uptake at higher latitudes compared to observations and other models, and do not resolve the transition in the flux at about 50° S as the other models.

The different patterns of annual uptake shown in Fig. 4 results in a broad range in the cumulative annual fluxes of CO$_2$ (Fig. 5). The cumulative fluxes from 75 to 58° S for the CCSM-BEC, CCSM-ETH and the CSIRO models are 0.0, $+0.06$ and $-0.04$ Pg C yr$^{-1}$, respectively, and are similar to the observation-based value of $+0.05$ Pg C yr$^{-1}$. The NEMO-Plankton5 and NEMO-PISCES models predict a greater sea–air CO$_2$ flux into the ocean from 75° S to 58° S of $-0.20$ and $-0.25$ Pg C yr$^{-1}$, respectively. A net flux of CO$_2$ to the atmosphere between about 50° S and 60° S (positive flux; Fig. 4) results in maxima in the cumulative sea–air flux of CO$_2$ at about 50° S for the CCSM-BEC and CCSM-ETH
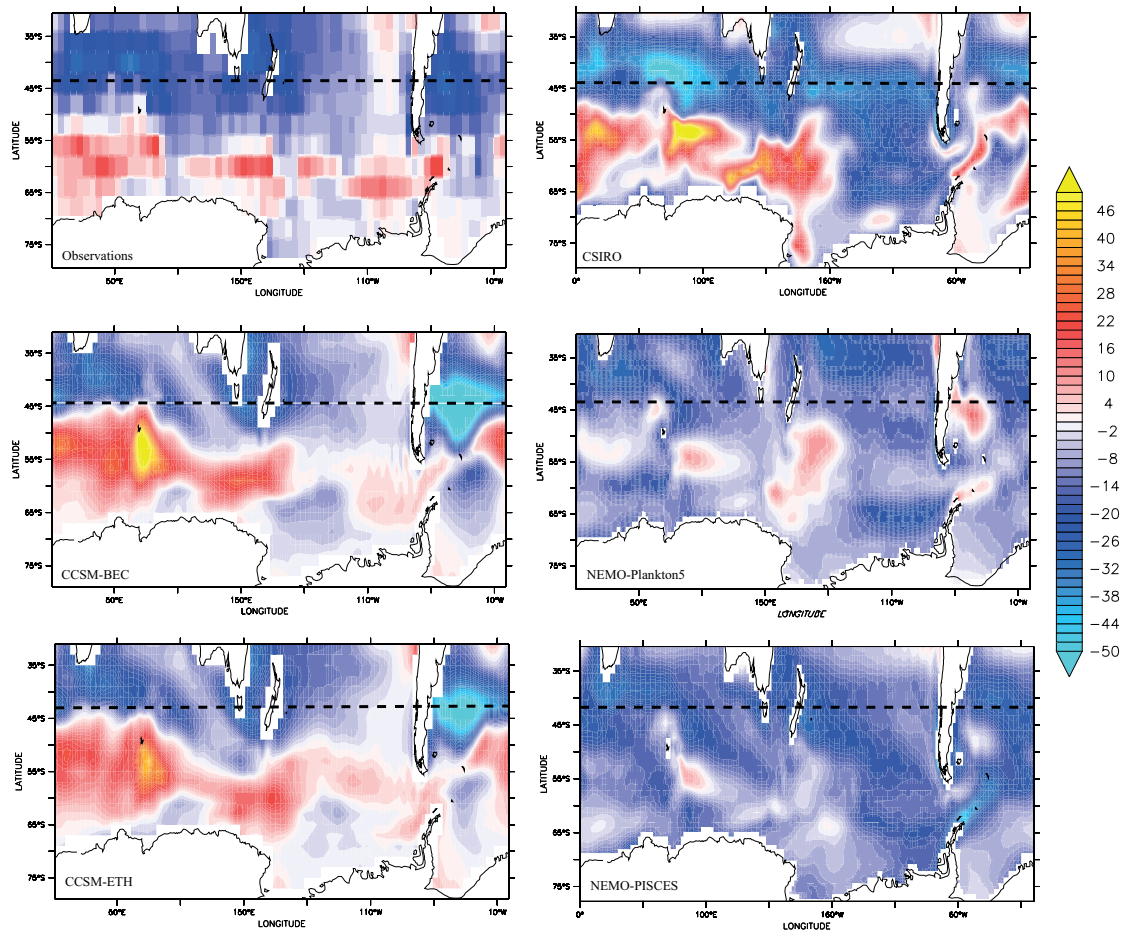
**Fig. 4.** Spatial maps of the annual mean uptake, in g C m$^{-2}$ yr$^{-1}$ from the five ocean biogeochemical models and observations; negative values reflect fluxes into the ocean. The dashed line represents the RECCAP boundary at 44° S.

models. This is only partially offset in these two models by uptake in the SAZ and the resulting net annual sea–air flux at 44° S is $-0.04$ Pg C yr$^{-1}$ (CCSM-BEC) and $+0.05$ Pg C yr$^{-1}$ (CCSM-ETH) compared to the observation based estimate of $-0.27$ Pg C yr$^{-1}$.

The CSIRO model also simulates regions of net flux to the atmosphere at high latitudes (Fig. 4), but these are largely offset by other zones of uptake in the same latitudinal range, resulting in only a slight maximum in the cumulative zonally integrated flux for this model near 50° S. A band of high CO$_2$ uptake in the Subantarctic and subtropical waters produces a cumulative uptake to 44° S of $-0.42$ Pg C yr$^{-1}$ for the CSIRO model. The cumulative uptake for both NEMO models increases to 44° S to $-0.4$ Pg C yr$^{-1}$ (NEMO-Plankton5) and $-0.8$ Pg C yr$^{-1}$ (NEMO-PISCES). The large deviation in the annual uptake for the ocean biogeochemical models appears to be in part due to how the sea–air CO$_2$ fluxes are simulated at latitudes poleward of 58° S (discussed in Sect. 3.1.3).

Atmospheric CO$_2$ inversions are usually constrained not only by the atmospheric CO$_2$ data, but also by a first guess or
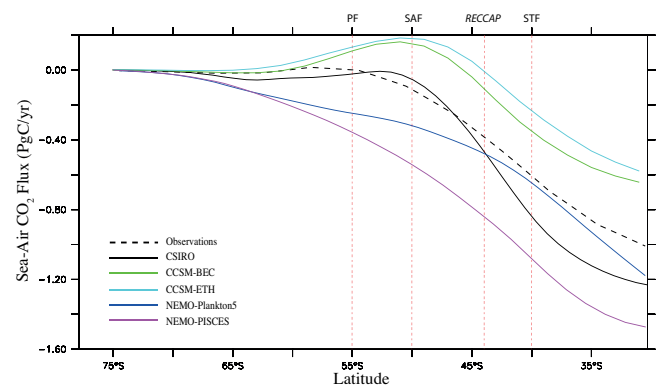


**Fig. 5.** The cumulative, zonally integrated, annual mean CO$_2$ uptake (30–75° S integrating from the south) from the biogeochemical ocean models and observations (dashed line) (Pg C yr$^{-1}$). Overlain are the nominal positions of the major Southern Ocean fronts and the RECCAP boundary at 44° S. Negative values reflect flux into the ocean.

a priori flux estimate. The estimated Southern Ocean flux was not very sensitive to this prior information; across inversions prior annual fluxes were clustered around $-0.35$ Pg C yr$^{-1}$ or $-1.0$ Pg C yr$^{-1}$, but this clustering is not maintained in the estimated fluxes from the inversions. This suggests that the observing network for this region may be sufficient to constrain the flux estimates. However, other differences between the inversions, such as the modelling of atmospheric transport, contribute to the range in atmospheric results. For example, a transport model with vigorous mixing of higher CO$_2$ concentration of air from the north would require a larger Southern Ocean sink to maintain the north–south gradient of CO$_2$ concentration than a transport model with slower mixing of air from the north.

The ocean inversions do not use a priori estimates, but they may be sensitive to biases in the data based techniques used to estimate the components of the observed dissolved inorganic carbon in the ocean due to anthropogenic carbon uptake and sea–air gas exchange (e.g. Matsumoto and Gruber, 2005; Gerber et al., 2009, 2010). Like atmospheric inversions, the ocean inversion is likely to be sensitive to biases in model transport, particularly in the Southern Ocean, but the use of a suite of different models has been employed to help quantify this uncertainty. Although ocean CO$_2$ inversions have been less widely used than atmospheric CO$_2$ inversions, this approach thus far seems to be relatively insensitive to the choice of inverse methodology (Gerber et al., 2010).

### 3.1.2 Southern Ocean, 44–58° S

The median annual sea–air flux values for the different approaches varies between $-0.26$ and $-0.35$ Pg C yr$^{-1}$ for the circumpolar region from 44 to 58° S. These values are similar to the annual uptake for the entire Southern Ocean (44–75° S), suggesting the majority of the net uptake occurs in this latitude band, consistent with previous studies (Metzl et al., 2006; McNeil et al., 2007; Takahashi et al., 2009, 2012).

The contributions of the Atlantic, Indian, and Pacific Ocean sectors to the annual uptake in the 44–58° S band are similar when all 26 models are grouped ($-0.13 \pm 0.04$, $-0.11 \pm 0.03$ and $-0.11 \pm 0.04$; Table 3). The ocean biogeochemical models and observations do suggest that greater uptake occurs in the Pacific sector, which is not apparent in the atmospheric or ocean inversion results.

It is important to note that the flux values for all approaches are associated with a large range, particularly ocean biogeochemical models (see Sect. 3.1.1) and atmospheric inversions. This is most evident in the Indian and southeast Pacific oceans where ocean biogeochemical models differ in the sign of the flux (Fig. 4). For atmospheric inversions, the basin split is dependent on the spatial resolution of the inversion; inversions that solve for only 1 or 2 regions rely on their prior information to determine the basin split, while inversions that

solve for many regions may be susceptible to "overfitting" the atmospheric measurements and thereby biasing the flux estimates. This may be a particular problem for the Southern Ocean as atmospheric CO$_2$ variations between observing stations are very small, placing high demands on data quality and a transport model's ability to represent that data. This is consistent with previous studies based on ocean inversions, which have shown that this approach cannot robustly separate the Indian and Pacific Ocean basins based available data (e.g. Mikaloff Fletcher et al., 2006, 2007).

### 3.1.3 Southern Ocean 58–75° S

The influence of this high latitude band (40 % of the total Southern Ocean surface area) on the annual sea–air CO$_2$ flux is small relative to the 44–58° S region, accounting for only about 10 % of the total Southern Ocean sea–air flux (Table 3). Ocean biogeochemical models and ocean inversions indicate that this region is a small net sink of atmospheric CO$_2$ annually ($-0.04 \pm 0.09$ and $-0.07 \pm 0.01$ Pg C yr$^{-1}$), with atmospheric inversions and observations suggesting a small net flux to the atmosphere ($+0.03 \pm 0.03$ and $+0.04 \pm 0.02$ Pg C yr$^{-1}$).

Ocean biogeochemical models again show the largest range in fluxes (Table 3 and Fig. 3). This variability may be due to (i) the representation of the sea ice and associated gas exchange differs across models (e.g. Rysgaard et al., 2011); and (ii) the coarse resolution of the models which precludes the proper representation of potentially important features such as polynas as well as other important coastal ocean processes (Marsland et al., 2004). This part of the Southern Ocean remains one of the most poorly sampled of all ocean regions (Fig. 2; Monteiro et al., 2010) and the uncertainty in the flux estimates based on observations may be underestimated.

This region was regarded as a strong annual sink of atmospheric CO$_2$ based on summer data (Takahashi et al., 2002), while more recent observations (Takahashi et al., 2009) have suggested that the higher latitude Southern Ocean is neutral or a weak source of atmospheric CO$_2$ over the annual mean. These estimates are based more on open-ocean observations rather than data collected in marginal seas and coastal margins of the Southern Ocean. These areas that have a high variability in biological production (e.g. Sweeney et al., 2000; Hales and Takahashi, 2004) and as a consequence have been suggested to play an important role in the global carbon budget (Arrigo et al., 2008). Amongst the approaches in this study, only atmospheric inversions have the potential to capture the integrated coastal, sea-ice and open-ocean responses in this region. That these inversions suggest that this region is not a large net sink of CO$_2$ suggests that either: (i) outgassing in the more northward portion of this region offsets any strong uptake, or (ii) the role of the coastal ocean and sea-ice zone is not well captured.
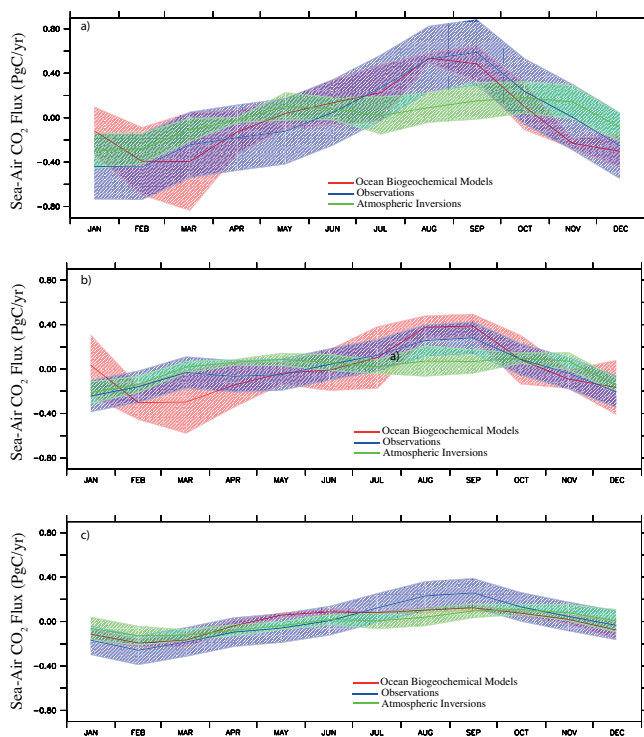
**Fig. 6.** Seasonal cycle anomaly of the Southern Ocean sea–air CO$_2$ flux (Pg C yr$^{-1}$) from observations, ocean biogeochemical and atmospheric inversions for the Southern Ocean (44–75° S; upper), the region 44–58° S (middle) and the region south of 58° S (lower). The shaded area represents the sea-air CO$_2$ flux uncertainty associated with each approach. Negative values reflect flux into the ocean.

## 3.2 Seasonal sea–air CO$_2$ fluxes

In this section we consider how the various modelling approaches represent the seasonality in the sea–air CO$_2$ exchange compared to observations. This provides insights into the ability of ocean biogeochemical models to represent the complex interplay of physical and biological processes that drive sea–air CO$_2$ exchange. The ability of a model to reproduce the seasonal cycle also provides some indication of the ocean biogeochemical models ability to correctly represent climate sensitive processes that could influence long-term projections of the ocean CO$_2$ uptake. The multi-model median seasonal anomalies of sea–air CO$_2$ fluxes are shown in Fig. 6, while the individual models and observations are shown in Fig. 7.

### 3.2.1 Southern Ocean 44–75° S

Figure 6a shows the median and MAD over the entire Southern Ocean RECCAP region. Some ocean biogeochemical models do simulate the seasonal cycle in the sea–air CO$_2$ flux estimated from observations (Figs. 6 and 7). In summer, a CO$_2$ flux into the ocean surface (negative flux) results from the combined effects of increased surface stratifi-
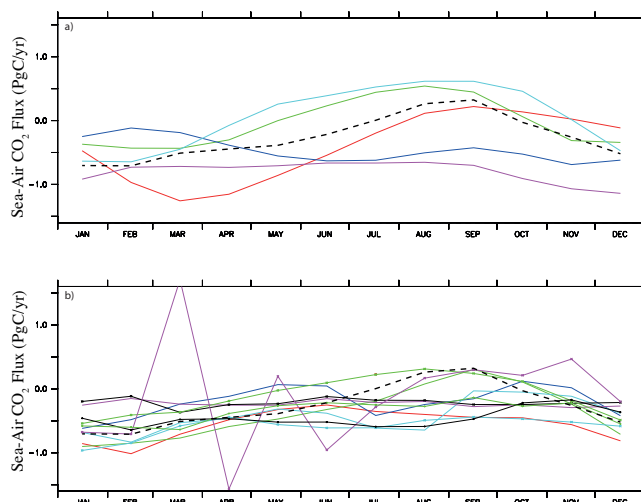


**Fig. 7.** The seasonal sea–air CO$_2$ fluxes for the Southern Ocean (44–75° S) from individual ocean biogeochemical models (upper) and individual atmospheric inverse estimates (lower). In both plots the observations are overlain (dashed black line). Negative values reflect flux into the ocean.

cation, warming, and increased biologically driven CO$_2$ uptake. Deeper mixing and lower production, offset to some degree by surface cooling, results in a reduced flux into the ocean and potential outgassing of CO$_2$ in winter (Takahashi et al., 2009). All approaches tend to give similar estimates in summer, but the atmospheric inversions do not capture the strong winter response evident in ocean models and estimated from observations.

To explore the relationship between the seasonal cycle and the annual mean uptake, we used a two-dimensional (2-D) Taylor Diagram (Fig. 8a). The annual mean uptake and timing of the seasonal flux changes relative to observationally based estimates were compared for each ocean biogeochemical model and atmospheric inversion. The analysis provides a synthesis of the ability of all models to capture the seasonal and annual sea–air fluxes. In this analysis, we do not account for the uncertainty associated with observationally derived fluxes, which are associated with large uncertainties (see Sect. 2.1.1).

The x-axis in each Taylor diagram is the normalized standard deviation of the seasonal cycle ($\sigma_{model}/\sigma_{obs}$); the closer the value is to 1 (denoted as a red arc in Fig. 8) the better it reproduces the magnitude of the seasonal cycle from the observations. The correlation of the model seasonal cycle with observations is shown on the arc; models or inversions with correlations of +1 (x-axis) will simulate the seasonality in the sea–air flux from observations. Models that lay in the right quadrant have positive correlation, while those in the left quadrant have negative, or anti-phase correlations. The colours of individual symbols represent the difference between the annual sea–air flux based on observations and the value for each model (i.e. observations − model/inversions).
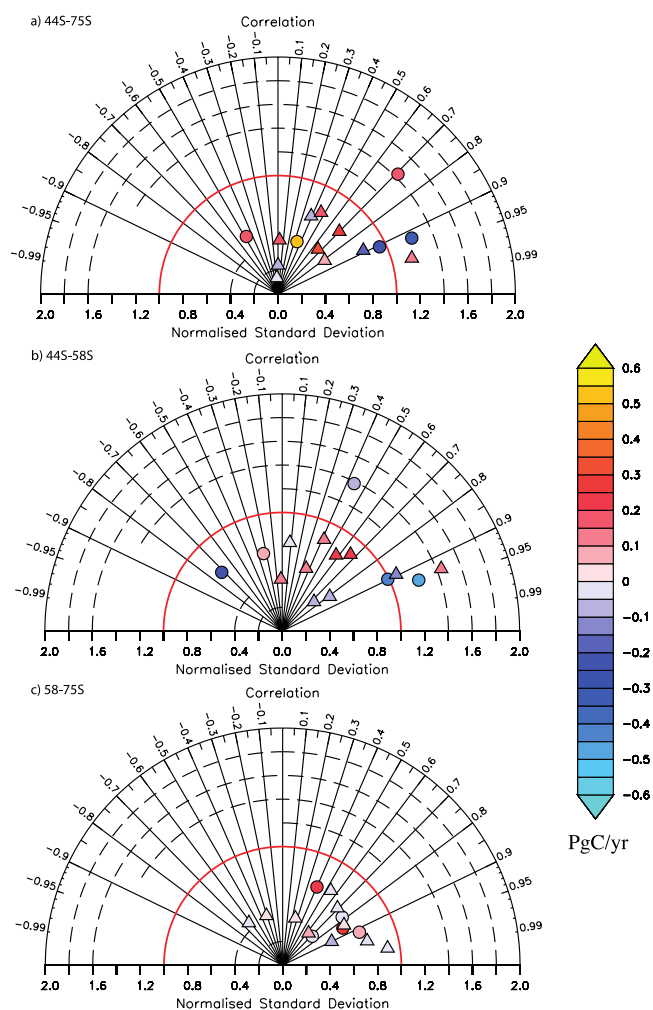
**Fig. 8.** Taylor diagram of the seasonal sea–air CO$_2$ flux assessed against the observations for ocean biogeochemical models (circles) and atmospheric inversion models (triangles). The upper panel represents the region 44–75° S; the middle panel the region 44–58° S; and the lower panel the region 58–75° S. The colours represent the difference between the total observed annual uptake and the models (see text for a comprehensive explanation). The annual mean differences (colour bar) are in Pg C yr$^{-1}$.

Ocean biogeochemical models are represented as circles, while triangles represent atmospheric inversions.

A diverse set of responses is evident in Fig. 8a. Many atmospheric inverse and ocean biogeochemical models underestimate the magnitude of the seasonal cycle. Several models and inversions appear to capture the magnitude and the phase of the seasonal cycle, however these models tend to strongly underestimate the magnitude of annual mean uptake (blue symbols with large negative values for the observations minus model difference). Some models and inversions do a poor job at capturing the phase of the seasonal cycle, but show better agreement in the annual mean uptake. These results are particularly worrisome, given that some models are unable

to simulate even the seasonality, which is the largest scale of variability in the Southern Ocean.

The reasons behind the poor seasonality in many atmospheric inversions remain unclear, but two factors may contribute. Firstly, the observed seasonality of atmospheric CO$_2$ in the Southern Ocean region is small, with roughly equal contributions from the seasonality of local ocean fluxes and from the transport of seasonal signals from sources and sinks in other regions. Due to the strong role of fluxes from distant regions in determining the seasonal cycle in atmospheric CO$_2$ at stations that observe the Southern Ocean, errors in the fluxes estimated from other regions or in the modelled transport of those fluxes to the high latitude southern hemisphere could lead to biases in the seasonal cycle. Secondly, some of the inversions that solve for smaller ocean regions (e.g. C13_CCAM_law) show very different seasonality between basins, suggesting some caution should be applied to those results. Possibly, the greater flexibility in those inversions to fit the atmospheric data makes them vulnerable to any data quality or representativeness issues as well as transport model errors. When inversions are solved for fewer regions, the inversion compromises the fit across sites effectively ignoring any poorly calibrated data. Conversely, inversions that solve for only a few regions could be missing important spatial variability in the seasonal cycle, which can lead to biases in the inverse estimates (Kaminski et al., 2001).

The representation of the seasonal cycle varies widely across the ocean biogeochemical models (Fig. 7). If the summer warming is too strong in the upper ocean, the solubility response can dominate over the biological productivity leading to a peak in the sea–air flux that is several months out of phase with observations (Fig. 8a). The net primary productivity from the models (not shown) has a similar magnitude over summer. This suggests that changes in the seasonal temperature and mixed layer depth are likely to be more important than the differences between biological models in causing the varied responses in the ocean models. Interestingly, capturing the seasonal cycle of the Southern Ocean is not a prerequisite to reproducing the annual mean sea–air flux calculated from observations. However, the inability of the models to simulate the observation-based seasonality in the sea–air CO$_2$ flux does bring into question the ability of these models to realistically project the response of the Southern Ocean CO$_2$ flux to climate change.

### 3.2.2 Southern Ocean 44–58° S

As with the entire Southern Ocean, the median seasonality for ocean biogeochemical models and observations agree in terms of the phase and magnitude of the seasonal cycle (Fig. 6b). The atmospheric inverse models simulate relatively weak seasonal amplitude. The similarity in the magnitude and phase with the total response (44–78° S) is consistent with this region dominating the seasonality in the sea–air flux

for the Southern Ocean (Metzl et al., 2006; Takahashi et al., 2009, 2012).

The 2-D Taylor diagram for individual models (Fig. 8b) shows a diverse range of responses. Some models represent the observation-based phase and magnitude of the seasonal cycle, but do a poor job in capturing the annual uptake. Some models that do approximately represent the annual uptake can display poorer magnitude and phase of the seasonal cycle. While individual models may not represent both the seasonal cycle and annual sea–air CO$_2$ flux, taking the median of multiple models (ensemble) agrees more favorably with the observed response.

### 3.2.3  Southern Ocean 58–75° S

At high latitudes, the magnitude of the seasonal cycle in the sea–air CO$_2$ flux is larger for fluxes derived from observations than for the ocean models and atmospheric inversions (Fig. 6c). While the annual median values (Table 3) are quite low in this region, observations indicate a relatively large summer flux into the ocean and a flux to the atmosphere in winter. Neither ocean biogeochemical models nor atmospheric inversions show a well-defined seasonal cycle. The atmospheric inversions show no evidence of a large summer CO$_2$ uptake (negative flux) associated with the coastal ocean and marginal seas as suggested by Arrigo et al. (2008).

The 2-D Taylor diagram showing the behaviour of the individual models for this region is shown in Fig. 8c. The biogeochemical models underestimate the seasonal cycle relative to observations, but most capture the observed phase and the models tend to agree on the magnitude of the seasonal cycle, explaining the small range of the ocean biogeochemical models in Fig. 6c. The smaller magnitude of the seasonal cycle in ocean biogeochemical models may well be related to the representation of the sea-ice zone as discussed in Sect. 3.1.3.

The atmospheric inversions show a diverse set of responses in this region. Consistent with the median, we see that the majority of these models underestimate the seasonal cycle relative to observations. Clearly most of the models do a good job capturing the phase of the seasonal cycle but do poorly at representing the annual mean uptake. However some models, while capturing the annual mean uptake well, show very little or poor seasonality. Some inversions produce a semi-annual cycle. These results again highlight that a well-represented seasonal cycle is not a prerequisite for capturing the annual mean uptake in atmospheric inverse models well. This is also confirmed by the negligible a posteriori correlations between seasonal anomalies and the mean in atmospheric inversions (e.g. Rödenbeck, 2005).

### 3.3  Longer-term variability

Understanding and quantifying interannual variability in the Southern Ocean is key to projecting the future response of

Southern Ocean sea–air fluxes. The detection of a long-term trend is difficult as observations tend to be most common in the austral summer and studies have shown that changes in sea surface temperature and net production can cause considerable variability in sea–air fluxes at regional scales during the summer months (Jabaud-Jan et al., 2004; Brévière et al., 2006; Borges et al., 2008; Brix et al., 2012). While a few observational studies attempt to describe the longer-term change of the carbon system, they focus on oceanic $p$CO$_2$ rather than changes in sea–air CO$_2$ fluxes (Inoue and Ishii, 2005; Lenton et al., 2012; Metzl, 2009; Midorikawa et al., 2012; Takahashi et al., 2009) or are station studies that may have local influences (Currie et al., 2009). Consequently, as we are focusing on sea–air CO$_2$ fluxes we only use atmospheric inversion and ocean biogeochemical models over the period 1990–2009, rather than observations.

### 3.3.1  Southern Ocean 44–75° S

The simulated median interannual variability and associated uncertainty in sea–air CO$_2$ fluxes from ocean biogeochemical models and atmospheric inverse models are shown in Fig. 9. The interannual variability in the period 1990–2009 from ocean biogeochemical models and atmospheric inversions are of similar maximum value (+0.10 and +0.11 Pg C yr$^{-1}$, respectively). This represents 20 % of the total median sea–air flux from ocean biogeochemical models and 35 % of the median flux from atmospheric inversions. The positive and negative flux anomalies are of similar magnitude.

The region 44–58° S can explain about 75 % of the interannual variability in the Southern Ocean sea–air CO$_2$ flux in the atmospheric inversions (+0.07 Pg C yr$^{-1}$) and ocean biogeochemical models (+0.08 Pg C yr$^{-1}$; Fig. 9b). The remaining 25 % of the interannual variability is attributable to the region 58–75° S (Fig. 9c). These results suggest that south of 58° S, the median interannual variability from ocean biogeochemical models (+0.03 Pg C yr$^{-1}$) and atmospheric inversions (+0.07 Pg C yr$^{-1}$) can be as large as the net annual sea–air CO$_2$ flux (Table 3). In this region the range in sea–air flux for ocean biogeochemical models is lower than in the atmospheric inverse models (consistent with Sect. 3.1.3). The large interannual variability poleward of 58° S may be due to biogeochemical responses to changes in heat and freshwater fluxes, wind stress and sea-ice cover. This could indicate that sea–air CO$_2$ fluxes in this region are more sensitive to climate than previously believed. The sea–air CO$_2$ fluxes in the 44–58° S and 58–75° S regions are correlated, which is consistent with the interannual variability being driven by large-scale Southern Ocean climate variability such as the Southern Annular Mode.

There are some common features across the atmospheric inversions and ocean biogeochemical models, e.g. most showing large ocean uptake in 2003. However, in the case of atmospheric inversions some caution is required as the
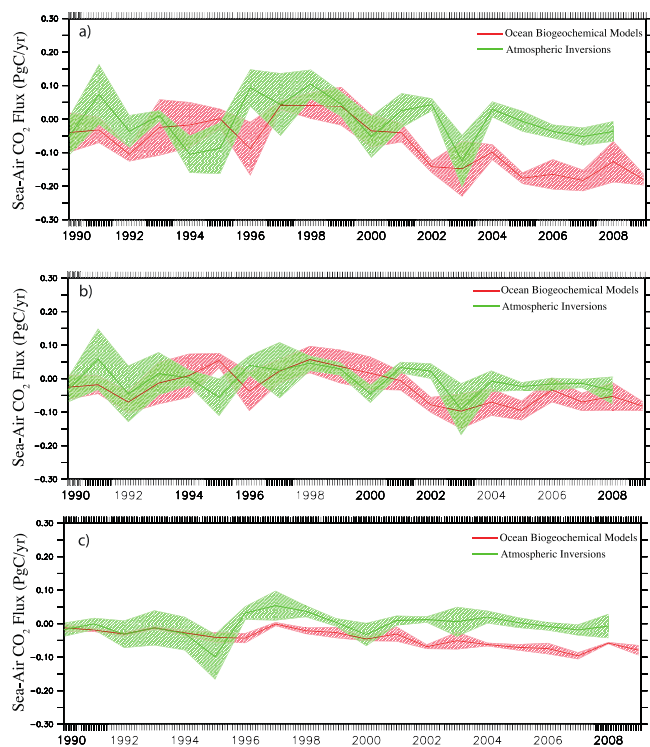
**Fig. 9.** The oceanic interannual variability in sea–air CO$_2$ flux from ocean biogeochemical and atmospheric inverse models in the period 1990–2009. The upper panel represents the region 44–75° S, the middle figure is the region 44–58° S and the lower region 58–75° S. The shaded area represents the sea–air CO$_2$ flux uncertainty associated with each approach. Negative values reflect flux into the ocean.
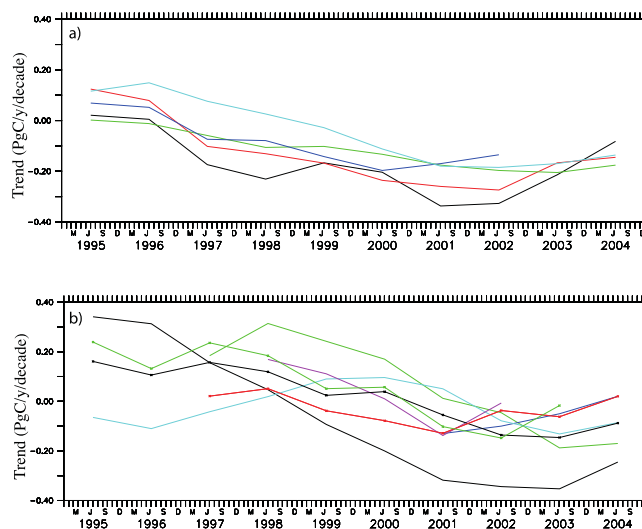


**Fig. 10.** Trends in ocean carbon uptake in the Southern Ocean between 44–75° S over different decadal periods (see text for explanation) in units of Pg C yr$^{-1}$ decade$^{-1}$. The upper panel shows the trends for individual ocean biogeochemical models and the lower panel shows the trends from individual atmospheric inverse models. Negative trend values reflect increasing flux into the ocean over each decadal period.

magnitude of these variations may well reflect over sensitivity to some of the atmospheric measurements. For example, the strong negative flux in 2003 may be driven by the atmospheric record at Jubany (58° W, 62° S), which has periods in 2003–2004 when the CO$_2$ concentration is 0.7–1.0 ppm lower than at nearby Palmer Station (64° W, 65° S). Consequently, those inversions that include this data give larger fluxes in 2003 than those that do not. It is interesting that this sensitivity occurs for inversions that span the range of flux resolution that the inversions solve for (i.e. one or many Southern Ocean regions). The positive and negative anomalies in 1997–1998 and 2000 are harder to attribute. Similar, though larger, anomalies are also seen for Southern Hemisphere land regions (Peylin et al., 2013, Fig. 6). This suggests that the atmospheric data may be insufficient to clearly differentiate land and ocean flux anomalies due to the usual practice of selecting atmospheric measurements to be representative of well-mixed air masses and thus removing data that has had recent contact with land.

The median of the ocean biogeochemical models shows a larger sea–air CO$_2$ flux in 2009 relative to the start of the study period in 1990 (Fig. 9). This is expected as the CO$_2$ gradient between the atmosphere and ocean has increased in

response to continuing atmospheric emissions of CO$_2$. The median of the atmospheric inversions shows no increase in CO$_2$ uptake over the study period. However, our confidence in these long-term trends is low, given the magnitude of the interannual variability and the relatively short period of simulations.

Figure 10a and b depict linear decadal trends computed as a function of time using a 10 yr sliding window centred on the reported year, following Lovenduski et al. (2008). The ocean biogeochemical models produce mostly negative trends, with the exception of decades centred in the mid-1990s. Atmospheric inversions in contrast show mostly a positive trend in the decades centred in the 1990s, and a negative trend from 2000 onwards; however, these trends are very variable both across inversions and within individual inversions, due to the large interannual variability in estimated fluxes (see Fig. 9a). Calculating the linear trend in Southern Ocean fluxes over the maximum period available from any given ocean biogeochemical model (18–20 yr) or inversion (13–19 yr and excluding those with less than 10 yr of output) yields a median and MAD trend of $-0.09 \pm 0.04$ Pg C yr$^{-1}$ decade$^{-1}$ for biogeochemical models and $0 \pm 0.03$ Pg C yr$^{-1}$ decade$^{-1}$ for the inversions. This enhanced uptake in ocean biogeochemical models is consistent with the expected uptake of $-0.05$ Pg C yr$^{-1}$ decade$^{-1}$ of the Southern Ocean sink (Le Quéré et al., 2007), due to the increasing atmospheric CO$_2$ concentration. Conversely, the inversions are more consistent with a reduction in the strength of the Southern Ocean sink reported by Le Quéré et al. (2007), but the range is

large across inversions ($-0.06$ to $0.08$ Pg C yr$^{-1}$ decade$^{-1}$) and previous work (Law et al., 2008) has shown that the inversion trends are likely quite sensitive to atmospheric CO$_2$ data quality, with atmospheric CO$_2$ gradients being close to measurement uncertainty (Stephens et al., 2013). This suggests that linear trends in model output over periods less than 20 yr are unlikely to provide a statistically meaningful statement about the very small changing rate of Southern Ocean CO$_2$ uptake. This is supported by the results of McKinley et al. (2011) for the North Atlantic.

## 4 Conclusion

The Southern Ocean, despite the important role it plays in the global carbon budget remains under sampled with respect to surface ocean carbon. In response to these limited observations, different approaches have been used to estimate total net sea–air CO$_2$ exchange of the Southern Ocean and understand different scales of variability: (i) synthesis of surface ocean observations; (ii) atmospheric inverse models; (iii) ocean inversions; and (iv) ocean biogeochemical models. The goal of this study is to combine these different approaches to quantify and assess how well the models represent the mean and variability of sea–air CO$_2$ fluxes in the Southern Ocean in comparison to flux estimates derived from observations. We used the recalculated sea–air CO$_2$ flux climatology of Wanninkhof et al. (2013) as our observational product: five different ocean biogeochemical models driven with observed atmospheric CO$_2$ concentrations; eleven atmospheric inverse models using atmospheric records collected around the Southern Ocean; and ten ocean inverse models.

Our results show that the median annual sea–air flux from all four approaches applied in the entire Southern Ocean region (44–75° S) is between $-0.27$ and $-0.43$ Pg C yr$^{-1}$, with a median value for all 26 models of $-0.42 \pm 0.07$ Pg C yr$^{-1}$. We see that the observation-based annual net uptake is nearly doubled to $-0.47$ Pg C yr$^{-1}$ if the boundary is shifted from 44 to 40° S, bringing the observations and ocean biogeochemical model results into closer agreement. The region 44–58° S dominates the annual flux with a median of all models of $-0.35 \pm 0.09$ Pg C yr$^{-1}$. Ocean biogeochemical models show the greatest mean absolute deviation in the modelled flux, which may be in part due to the RECCAP boundary at 44° S and the proportion of the important SAZ included in this calculation. In the region south of 58° S, both ocean biogeochemical models and ocean inversions show a small net CO$_2$ flux into the ocean (negative flux), while atmospheric inversions and estimates from observations show a small net flux to the atmosphere (positive flux). We see little evidence in the atmospheric inversions for the strong sink of CO$_2$ suggested by Arrigo et al. (2008) for this region.

The choice of the RECCAP boundary at 44° S was problematic in comparing our results with published values from

other studies (e.g. Metzl et al., 1999; Boutin et al., 2008; Mc-Neil et al., 2007; Barbero et al., 2011; Takahashi et al., 2012). Therefore, while we focused on the comparison between the four different techniques presented here, a more comprehensive analysis of individual regions needs to be undertaken in future studies. Such studies would be timely, particularly in light of recent work highlighting the heterogeneity of the anthropogenic carbon transport out of the Southern Ocean (Sallee et al., 2012).

At seasonal times scales, the fluxes estimated from observations and the median of the ocean biogeochemical models capture a well-defined seasonal cycle in the sea–air CO$_2$ flux. Atmospheric inversions showed only very weak or little seasonality in all regions of the Southern Ocean. All approaches tend to show enhanced flux into the ocean in the biologically productive summer period. The largest seasonality was found in the region 44–58° S for both ocean biogeochemical models and based on observations. South of 58° S, neither ocean biogeochemical models nor atmospheric inversions were able to capture the magnitude of the observed seasonal cycle. These differences between models and observational estimates may reflect the model formulation and a poor understanding of the high latitude carbon cycle. None of the models were capable of simulating the magnitude and phase of seasonality and the annual mean sea–air flux at the same time in any of the regions. This raises serious concerns about projecting the future changes in Southern Ocean CO$_2$ uptake.

Interannually, ocean models and atmospheric inversions show that the variability in the Southern Ocean sea–air CO$_2$ flux can be as large as 25 % of the annual mean. Atmospheric inversions tend to produce a larger spread in the interannual variability of the sea–air flux than ocean biogeochemical models. Both modelling approaches suggest that about 25 % of the total interannual variability can be explained by the region south of 58° S. This implies that this variability can be as large as the net annual mean sea–air CO$_2$ flux in this region.

Resolving long-term trends is difficult due to the large interannual variability and the short time frame (1990–2009) of this study; this is particularly evident from the large spread in trends from ocean biogeochemical models and inversions. Reliable detection of Southern Ocean trends from atmospheric inversions requires careful assessment of the atmospheric CO$_2$ measurements input to inversions and their calibration over time; the provision of high quality atmospheric datasets from remote locations in the Southern Ocean is both challenging and vital. Nevertheless, in the period 1990–2009 atmospheric inversions do suggest little change in the strength of the CO$_2$ sink broadly consistent with the results of Le Quéré et al. (2007). In contrast, ocean biogeochemical models show increasing oceanic uptake consistent with the expected increase of $-0.05$ Pg C yr$^{-1}$ decade$^{-1}$ (Le Quéré et al., 2007) due to increasing atmospheric CO$_2$.

Of all the approaches in this paper, it is only ocean biogeochemical models that are prognostic in nature. If we are

to have confidence in the projections of Southern Ocean sea–air fluxes of CO$_2$, it is important that the models used to understand the response of the carbon cycle over the historical period not only capture the annual mean flux but also the seasonal cycle associated with this flux. Potentially, techniques such as water mass analysis may play an important role in helping understand the behaviour of the Southern Ocean carbon cycle (Iudicone et al., 2011). Such models are the integration of all of our knowledge and our ability to reproduce observations remains a key test of our understanding of the earth system (Falkowski et al., 2000).

Edited by: P. Ciais

# References

Arrigo, K. R., van Dijken, G., and Long, M.: Coastal Southern Ocean: A strong anthropogenic CO$_2$ sink, Geophys. Res. Lett., 35, L21602, doi:10.1029/2008gl035624, 2008.

Atlas, R., Hoffman, R. N., Ardizzone, J., Leidner, S. M., Jusem, J. C., Smith, D. K., and Gombos, D.: A Cross-Calibrated Multiplatform Ocean Surface Wind Velocity Product for Meteorological and Oceanographic Applications, B Am. Meteor. Soc., 92, 157–174, doi:10.1175/2010bams2946.1, 2011.

Aumont, O. and Bopp, L.: Globalizing results from ocean in situ iron fertilization studies, Global Biogeochem. Cy., 20, doi:10.029/2005GB002519, 2006.

Baker, D. F., Law, R. M., Gurney, K. R., Rayner, P., Peylin, P., Denning, A. S., Bousquet, P., Bruhwiler, L., Chen, Y. H., Ciais, P., Fung, I. Y., Heimann, M., John, J., Maki, T., Maksyutov, S., Masarie, K., Prather, M., Pak, B., Taguchi, S., and Zhu, Z.: TransCom 3 inversion intercomparison: Impact of transport model errors on the interannual variability of regional CO$_2$ fluxes, 1988–2003, Global Biogeochem. Cy., 20, GB1002, doi:10.1029/2004gb002439, 2006.

Bakker, D. C. E., Hoppema, M., Schröder, M., Geibert, W., and de Baar, H. J. W.: A rapid transition from ice covered CO$_2$-rich waters to a biologically mediated CO$_2$ sink in the eastern Weddell Gyre, Biogeosciences, 5, 1373–1386, doi:10.5194/bg-5-1373-2008, 2008.

Barbero, L., Boutin, J., Merlivat, L., Martin, N., Takahashi, T., Sutherland, S. C., and Wanninkhof, R.: Importance of water mass formation regions for the air-sea CO$_2$ flux estimate in the Southern Ocean, Global Biogeochemical Cy., 25, GB1005, doi:10.1029/2010gb003818, 2011.

Borges, A. V., Tilbrook, B., Metzl, N., Lenton, A., and Delille, B.: Inter-annual variability of the carbon dioxide oceanic sink south of Tasmania, Biogeosciences, 5, 14–155, doi:10.5194/bg-5-141-2008, 2008.

Boutin, J., Merlivat, L., Henocq, C., Martin, N., and Sallee, J. B.: Air-sea CO$_2$ flux variability in frontal regions of the Southern Ocean from CARbon Interface OCean Atmosphere drifters, Limnol. Oceanogr., 53, 2062–2079, 2008.

Brévière, E., Metzl, N., Poisson, A., and Tilbrook, B.: Changes of the oceanic CO$_2$ sink in the Eastern Indian sector of the Southern Ocean, Tellus B, 52, 438–446, 2006.

Brix, H., Currie, K. I., and Mikaloff Fletcher, S. E.: Seasonal variability of the carbon cycle in subantarctic surface water in the South West Pacific, Global Biogeochem. Cy., 27, 200–211, doi:10.1002/gbc.20023, 2013.

Caldeira, K. and Duffy, P. B.: The role of the Southern Ocean in uptake and storage of anthropogenic carbon dioxide, Science, 287, 620–622, 2000.

Canadell, J. G., Ciais, P., Gurney, K., Le Quéré, C., Piao, S., Raupach, M. R., and Sabine, C.: An international effort to to quantify regional carbon fluxes, EOS, 92, 81–82, 2011.

Chevallier, F., Ciais, P., Conway, T. J., Aalto, T., Anderson, B. E., Bousquet, P., Brunke, E. G., Ciattaglia, L., Esaki, Y., Frohlich, M., Gomez, A., Gomez-Pelaez, A. J., Haszpra, L., Krummel, P. B., Langenfelds, R. L., Leuenberger, M., Machida, T., Maignan, F., Matsueda, H., Morgui, J. A., Mukai, H., Nakazawa, T., Peylin, P., Ramonet, M., Rivier, L., Sawa, Y., Schmidt, M., Steele, L. P., Vay, S. A., Vermeulen, A. T., Wofsy, S., and Worthy, D.: CO$_2$ surface fluxes at grid point scale estimated from a global 21 year reanalysis of atmospheric measurements, J. Geophys. Res.-Atmos., 115, D21307, doi:10.1029/2010jd013887, 2010.

Currie, K. I,, Reid, M., and Hunter, K. A.: Interannual variability of carbon dioxide drawdown by subantarctic surface water near New Zealand, Biogeochemistry, 104, 23–34, doi:10.1007/s10533-009-9355-3, 2009.

Falkowski, P., Scholes, R. J., Boyle, E., Canadell, J., Canfield, D., Elser, J., Gruber, N., Hibbard, K., Hogberg, P., Linder, S., Mackenzie, F. T., Moore, B., Pedersen, T., Rosenthal, Y., Seitzinger, S., Smetacek, V., and Steffen, W.: The global carbon cycle: A test of our knowledge of earth as a system, Science, 290, 291–296, 2000.

Gauss, C. F.: Bestimmung der Genauigkeit der Beobachtungen, Zeitschrift für Astronomie und verwandt Wissenschaften, 1, 187–197, 1816

Gerber, M. and Joos, F.: Carbon sources and sinks from an Ensemble Kalman Filter ocean data assimilation, Global Biogeochem. Cy., 24, GB3004, doi:10.1029/2009GB003531, 2010.

Gerber, M., Joos, F., Vazquez-Rodriguez, M., Touratier, F., and Goyet, C.: Regional air-sea fluxes of anthropogenic carbon inferred with an Ensemble Kalman Filter, Global Biogeochem. Cy., 23, GB1013, doi:10.1029/2008GB003247, 2009.

Geider, R. J., H. L. MacIntyre, H. L., and Kana, T. M.: Dynamic model of phytoplankton growth and acclimation: responses of the balanced growth rate and the chlorophyll a:carbon ratio to light, nutrient-limitation and temperature, Mar. Ecol.-Prog. Ser., 148, 187–200, 1997

GLOBALVIEW-CO$_2$: Cooperative Atmospheric Data Integration Project – Carbon Dioxide, CD-ROM, NOAA ESRL, Boulder, Colorado [Also available on Internet via anonymous FTP to ftp.cmdl.noaa.gov, path: ccg/co2/GLOBALVIEW/gvco2, 2011.

Graven, H. D., Gruber, N., Key, R. M., Khatiwala, S., and Giraud, X.: Changing controls on oceanic radiocarbon: New insights on shallow-to-deep ocean exchange and anthropogenic CO$_2$ uptake, J. Geophys. Res.-Oceans, 117, C10005, doi:10.1029/2012JC008074, 2012.

Gruber, N.: Carbon Cycle Fickle Trends in the Ocean, Nature, 458, 155–156, doi:10.1038/458155a, 2009.

Gruber, N., Gloor, M., Fletcher, S. E. M., Doney, S. C., Dutkiewicz, S., Follows, M. J., Gerber, M., Jacobson, A. R., Joos, F., Lindsay, K., Menemenlis, D., Mouchet, A., Muller, S. A., Sarmiento, J. L., and Takahashi, T.: Oceanic sources, sinks, and transport of atmospheric CO$_2$, Global Biogeochem. Cy., 23, GB1005, doi:10.1029/2008gb003349, 2009.

Hales, B. and Takahashi, T.: High-resolution biogeochemical investigation of the Ross Sea, Antarctica, during the AESOPS (U. S. JGOFS) Program, Global Biogeochem. Cy., 18, GB3006, doi:10.1029/2003GB002165, 2004.

Inoue, H. Y. and Ishii, M.: Variations and trends of CO$_2$ in the surface seawater in the Southern Ocean south of Australia between 1969 and 2002, Tellus B, 57, 58–69, 2005.

Ishii, M., Inoue, H. Y., Matsueda, H., and Tanoue, E.: Close coupling between seasonal biological production and dynamics of dissolved inorganic carbon in the Indian Ocean sector and the western Pacific Ocean sector of the Antarctic Ocean, Deep-Sea Res. Pt. I, 45, 1187–1209, 1998.

Ishii, M., Inoue, H. Y., and Matsueda, H.: Net community production in the marginal ice zone and its importance for the variability of the oceanic $p$CO$_2$ in the Southern Ocean south of Australia, Deep-Sea Res. Pt. II, 49, 1961–1706, 2002.

Iudicone, D., Rodgers, K. B., Stendardo, I., Aumont, O., Madec, G., Bopp, L., Mangoni, O., and Ribera d'Alcala', M.: Water masses as a unifying framework for understanding the Southern Ocean Carbon Cycle, Biogeosciences, 8, 103–1052, doi:10.5194/bg-8-1031-2011, 2011.

Jabaud-Jan, A., Metzl, N., Brunet, C., Poisson, A., and Schauer, B.: Interannual varaibility of the carbon dioxide system in the southern Indian Ocean (20°–60° S): the impact of a warm anomaly in the austral summer 1998, Global Biogeochemical Cy., 18, GB1042, doi:1010.1029/2002GB002017, 2004.

Kaminski, T., Rayner, P. J., Heimann, M., and Enting, I. G.: On aggregation errors in atmospheric transport inversions, J. Geophys. Res., 106, 4703–4715, 2001.

Law, R. M., Matear, R. J., and Francey, R. J.: Comment on "Saturation of the Southern Ocean CO$_2$ sSink Due to Climate Change", Science, 319, p. 570, doi:10.1126/science.1149077, 2008.

Lenton, A. and Matear, R. J.: The role of the Southern Annular Mode (SAM) in Southern Ocean CO$_2$ uptake, Global Biogeochem. Cy., 21, GB2016, doi:10.1029/2006GB002714, 2007.

Lenton, A., Matear, R. J., and Tilbrook, B.: Observational Strategy to Constrain the Annual Air-Sea Flux of CO$_2$ in the Southern Ocean, Global Biogeochem. Cy., 20, doi:10,1029/GB002620, 2006.

Lenton, A., Codron, F., Bopp, L., Metzl, N., Cadule, P., Tagliabue, A., and Le Sommer, J.: Stratospheric ozone depletion reduces ocean carbon uptake and enhances ocean acidification, Geophys. Res. Lett., 36, L12606, doi:10.1029/2009gl038227, 2009.

Lenton, A., Metzl, N., Takahashi, T., Kuchinke, M., Matear, R. J., Roy, T., Sutherland, S. C., Sweeney, C., and Tilbrook, B.: The observed evolution of oceanic $p$CO$_2$ and its drivers over the last two decades, Global Biogeochem. Cy., 26, GB2021, doi:10.1029/2011gb004095, 2012.

Le Quéré, C., Rodenbeck, C., Buitenhuis, E. T., Conway, T. J., Langenfelds, R., Gomez, A., Labuschagne, C., Ramonet, M., Nakazawa, T., Metzl, N., Gillett, N., and Heimann, M.: Saturation of the Southern Ocean CO$_2$ Sink Due to Recent Climate Change, Science, doi:10.1126/science.1136188, 316, 1735–1738, 2007.

Le Quéré, C., Raupach, M. R., Canadell, J. G., Marland, G., Bopp, L., Ciais, P., Conway, T. J., Doney, S. C., Feely, R. A., Foster, P., Friedlingstein, P., Gurney, K., Houghton, R. A., House, J. I., Huntingford, C., Levy, P. E., Lomas, M. R., Majkut, J., Metzl, N., Ometto, J. P., Peters, G. P., Prentice, I. C., Randerson, J. T., Running, S. W., Sarmiento, J. L., Schuster, U., Sitch, S., Takahashi, T., Viovy, N., van der Werf, G. R., and Woodward, F. I.: Trends in the sources and sinks of carbon dioxide, Nat. Geosci., 2, 831–836, doi:10.1038/Ngeo689, 2009.

Loose, B. and Schlosser, P.: Sea ice and its effect on CO$_2$ flux between the atmosphere and the Southern Ocean interior, J. Geophys. Res.-Oceans, 116, C11019, doi:10.1029/2010jc006509, 2011.

Lovenduski, N., Gruber, N., Doney, S. C., and Lima, I. D.: Enhanced CO$_2$ outagssing in the Southern Ocean from a positive phase of the Southern Annular Mode, Global Biogeochem. Cy., 21, GB2026. doi:10.1029/2006GB002900, 2007.

Lovenduski, N. S., Gruber, N., and Doney, S. C.: Toward a mechanistic understanding of the decadal trends in the Southern Ocean carbon sink, Global Biogeochem. Cy., 22, GB3016, doi:10.1029/2007gb003139, 2008.

Maki, T., Ikegami, M., Fujita, T., Hirahara, T., Yamada, K., Mori, K., Takeuchi, A., Tsutsumi, Y., Suda, K., and Conway, T. J.: New technique to analyse global distributions of CO$_2$ concentrations and fluxes from non-processed observational data, Tellus B, 62, 797–809, doi:10.1111/J.1600-0889.2010.00488.X, 2010.

Marsland, S. J., Bindoff, N. L. D., Williams W. G., and Budd, W. F.: Modelling water mass formation in the Mertz Glacier Polynya and Adelie Depression, J. Geophys. Res., 109, C11003, doi:10.1029/2004JC002441, 2004.

Matear, R. J. and Lenton, A.: Impact of Historical Climate Change on the Southern Ocean Carbon Cycle, J. Climate, 21, 5820–5834, doi:10.1175/2008JCLI2194.1, 2008.

Matsumoto, K. and Gruber, N.: How accurate is the estimation of anthropogenic carbon in the ocean? An evaluationof the $\Delta$C* method, Global Biogeochem. Cy., 19, doi:10.1029/2004GB002397, 2005.

McKinley, G. A., Fay, A. R., Takahashi, T., and Metzl, N.: Convergence of atmospheric and North Atlantic carbon dioxide trends on multidecadal timescales, Nat. Geosci., 4, 606–610, doi:10.1038/Ngeo1193, 2011.

McNeil, B. I., Metzl, N., Key, R. M., Matear, R. J and Corbiere, A.: An empirical estimate of the Southern Ocean air-sea CO$_2$ flux, Global Biogeochem. Cy., GB3011, doi:10.1029/2007GB002991, 2007.

Metzl, N.: Decadal increase of oceanic carbon dioxide in Southern Indian Ocean surface waters (1991–2007), Deep-Sea Res Pt. II, 56, 607–619, doi:10.1016/J.Dsr2.2008.12.007, 2009.

Metzl, N., Tilbrook, B., and Poisson, A.: The annual $f$CO$_2$ cycle and the air-sea CO$_2$ flux in the sub-Antarctic Ocean, Tellus B, 51, 849–861, 1999.

Metzl, N., Brunet, C., Jabaud-Jan A., Poisson, A., and Schauer, B.: Summer and winter air-sea CO$_2$ fluxes in the Southern Ocean Deep Sea Res Pt. I, 53, 1548–1563, doi:10.1016/j.dsr.2006.07.006, 2006.

Midorikawa, T., Inoue, H. Y., Ishii, M., Sasano, D., Kosugi, N., Hashida, G., Nakaoka, S., and Suzuki, T.: Decreasing pH trend estimated from 35-year time series of carbonate parameters in the Pacific sector of the Southern Ocean in summer, Deep-Sea Res. Pt. I, 61, 131–139, 2012.

Mikaloff Fletcher, S. E., Gruber, N., Jacobson, A. R., Doney, S. C., Dutkiewicz, S., Gerber, M., Follows, M., Joos, F., Lindsay, K., Menemenlis, D., Mouchet, A., Muller, S. A., and Sarmiento, J. L.: Inverse estimates of anthropogenic CO$_2$ uptake, transport, and storage by the ocean, Global Biogeochem. Cy., 21, GB1010, doi:10.1029/2006GB002751, 2006.

Mikaloff Fletcher, S. E., Gruber, N., Jacobson, A. R., Gloor, M., Doney, S. C., Dutkiewicz, S., Gerber, M., Follows, M., Joos, F., Lindsay, K., Menemenlis, D., Mouchet, A., Muller, S. A., and Sarmiento, J. L.: Inverse estimates of the oceanic sources and sinks of natural CO$_2$ and the implied oceanic carbon transport, Global Biogeochem. Cy., 21, GB1010, doi:10.1029/2006gb002751, 2007.

Monteiro, P. M. S., Schuster, U., Hood, M., Lenton, A., Metzl, N., Olsen, A., Rogers, K., Sabine, C., Takahashi, T., Tilbrook, B., Yoder, J., Wanninkhof, R., Watson, A., and 2009: A global sea surface carbon observing system: assessment of changing sea surface CO$_2$ and air-sea CO$_2$ fluxes, in: Proceedings of the "OceanObs'09: Sustained Ocean Observations and Information for Society" Conference, Venice, Italy, 21-25 September 2009, ESA Publication WPP-306, 2010: A global sea surface carbon observing system: assessment of changing sea surface CO$_2$ and air-sea CO$_2$ fluxes, edited by: Hall, J., Harrison D. E., and Stammer, D., OceanObs'09: Sustained Ocean Observations and Information for Society, Venice, Italy, 2010.

Niwa, Y., Machida, T., Sawa, Y., Matsueda, H., Schuck, T. J., Brenninkmeijer, C. A. M., Imasu, R., and Satoh, M.: Imposing strong constraints on tropical terrestrial CO$_2$ fluxes using passenger aircraft based measurements, J. Geophys. Res.-Atmos., 117, D11303, doi:10.1029/2012jd017474, 2012.

Orsi, A. H., Whitworth III, T., and Nowlin Jr., W. D.: On the meridional extent and fronts of the Antarctic Circumpolar Current, Deep-Sea Res. Pt. I, 42, 641–673, 1995.

Patra, P. K., Maksyutov, S., Ishizawa, M., Nakazawa, T., Takahashi, T., and Ukita, J.: Interannual and decadal changes in the sea–air CO$_2$ flux from atmospheric CO$_2$ inverse modeling, Global Biogeochem. Cy., 19, GB4013, doi:10.1029/2004gb002257, 2005.

Peters, W., Jacobson, A. R., Sweeney, C., Andrews, A. E., Conway, T. J., Masarie, K., Miller, J. B., Bruhwiler, L. M. P., Petron, G., Hirsch, A. I., Worthy, D. E. J., van der Werf, G. R., Randerson, J. T., Wennberg, P. O., Krol, M. C., and Tans, P. P.: An atmospheric perspective on North American carbon dioxide exchange: CarbonTracker, P. Natl. Acad. Sci. USA, 104, 18925–18930, doi:10.1073/Pnas.0708986104, 2007.

Peters, W., Krol, M. C., van der Werf, G. R., Houweling, S., Jones, C. D., Hughes, J., Schaefer, K., Masarie, K. A., Jacobson, A. R., Miller, J. B., Cho, C. H., Ramonet, M., Schmidt, M., Ciattaglia, L., Apadula, F., Helta, D., Meinhardt, F., di Sarra, A. G., Piacentino, S., Sferlazzo, D., Aalto, T., Hatakka, J., Strom, J., Haszpra, L., Meijer, H. A. J., van der Laan, S., Neubert, R. E. M., Jordan, A., Rodo, X., Morgui, J. A., Vermeulen, A. T., Popa, E., Rozanski, K., Zimnoch, M., Manning, A. C., Leuenberger, M., Uglietti, C., Dolman, A. J., Ciais, P., Heimann, M., and Tans, P. P.: Seven years of recent European net terrestrial carbon dioxide exchange constrained by atmospheric observations, Glob. Change Biol., 16, 1317–1337, doi:10.1111/J.1365-2486.2009.02078.X, 2010.

Peylin, P., Law, R. M., Gurney, K. R., Chevallier, F., Jacobson, A. R., Maki, T., Niwa, Y., Patra, P. K., Peters, W., Rayner, P. J., Rödenbeck, C., and Zhang, X.: Global atmospheric carbon budget: results from an ensemble of atmospheric CO2 inversions, Biogeosciences Discuss., 10, 5301–5360, doi:10.5194/bgd-10-5301-2013, 2013.

Piao, S., Fang, J., Ciais, P., Peylin, P., Huang, Y., Sitch, S., and Wang, T.: The carbon balance of terrestrial ecosystems in China, Nature, 458, 1009–1013, doi:10.1038/nature07944, 2009.

Rayner, P. J., Law, R. M., Allison, C. E., Francey, R. J., Trudinger, C. M., and Pickett-Heaps, C.: Interannual variability of the global carbon cycle (1992-2005) inferred by inversion of atmospheric CO$_2$ and $\delta^{13}$CO$_2$ measurements, Global Biogeochem. Cy., 22, GB3008, doi:10.1029/2007gb003068, 2008.

Rödenbeck, C.: Estimating CO$_2$ sources and sinks from atmospheric mixing ratio measurements using a global inversion of atmospheric transport, Max Planck Institute for Biogeochemistry, Jena, 2005.

Roy, T., Rayner, P. J., Matear, R. J., and Francey, R.: Southern hemisphere ocean CO$_2$ uptake: reconciling atmospheric and oceanic estimates, Tellus B, 55, 701–710, 2003.

Roy, T., Bopp, L., Gehlen, M., Schneider, B., Cadule, P., Frolicher, T. L., Segschneider, J., Tjiputra, J., Heinze, C., and Joos, F.: Regional impacts of climate change and atmospheric CO$_2$ on future ocean carbon uptake: A multimodel linear feedback analysis, J. Climate, 24, 5195–5195, doi:10.1175/Jcli-D-11-00285.1, 2011.

Rysgaard, S., Bendtsen, J., Delille, B., Dieckmann, G. S., Glud, R. N., Kennedy, H., Mortensen, J., Papadimitriou, S., Thomas, D. N., and Tison, J. L.: Sea ice contribution to the air-sea CO$_2$ exchange in the Arctic and Southern Oceans, Tellus B, 63, 823–830, doi:10.1111/J.1600-0889.2011.00571.X, 2011.

Sallee, J. B., Matear, R. J., Rintoul, S. R., and Lenton, A.: Localized subduction of anthropogenic carbon dioxide in the Southern Hemisphere oceans, Nat. Geosci., 5, 579–584, doi:10.1038/Ngeo1523, 2012.

Sarmiento, J. L., Gruber, N., Brzezinski, M. A., and Dunne, J. P.: High-latitude Controls of Thermocline Nutrients and Low Latitude Biological Productivity, Nature, 427, 56–60, 2004.

Schuster, U., McKinley, G. A., Bates, N., Chevallier, F., Doney, S. C., Fay, A. R., González-Dávila, M., Gruber, N., Jones, S., Krijnen, J., Landschützer, P., Lefèvre, N., Manizza, M., Mathis, J., Metzl, N., Olsen, A., Rios, A. F., Rödenbeck, C., Santana-Casiano, J. M., Takahashi, T., Wanninkhof, R., and Watson, A. J.: An assessment of the Atlantic and Arctic sea–air CO$_2$ fluxes, 1990–2009, Biogeosciences, 10, 607–627, doi:10.5194/bg-10-607-2013, 2013.

Sokolov, S.: Chlorophyll blooms in the Antarctic Zone south of Australia and New Zealand in reference to the Antarctic Circumpolar Current fronts and sea ice forcing, J. Geophys. Res.-Oceans, 113, C03022, doi:10.1029/2007jc004329, 2008.

Stephens, B. B., Brailsford, G. W., Gomez, A. J., Riedel, K., Mikaloff Fletcher, S. E., Nichol, S., and Manning, M.: Analysis of a 39-year continuous atmospheric CO$_2$ record from Baring Head, New Zealand, Biogeosciences, 10, 2683–2697, doi:10.5194/bg-10-2683-2013, 2013.

Sweeney, C., Gloor, E., Jacobson, A. R., Key, R. M., McKinley, G., Sarmiento, J. L., and Wanninkhof, R.: Constraining global air-sea gas exchange for CO$_2$ with recent bomb C-14 measurements, Global Biogeochem. Cy., 21, Gb2015, doi:10.1029/2006gb002784, 2007.

Sweeney, C., Hansell, D. A., Carlson, C. A., Codispoti, L. A., Gordon, L. I., Marra, J., Millero, F. J., Smith, W. O., and Takahashi, T.: Biogeochemical regimes, net community production and carbon export in the Ross Sea, Antarctica, Deep-Sea Res. Pt. II, 47, 3369–3394, 2000.

Takahashi, T., Feely, R. A., Weiss, R., Wanninkhof, R. H. Chipman, D. W. Sutherland, S. C., and Takahashi, T. T.: Global air–sea flux of CO$_2$: an estimate based on measurements of sea–air $p$CO$_2$ difference, P. Natl. Acad. Sci., 94, 8292–8299, 1997.

Takahashi, T., Sutherland, S. C., Sweeney, C., Poisson, A., Metzl, N., Tilbrook, B., Bates, N., Wanninkhof, R., Feely, R. A., Sabine, C., Olafsson, J., and Nojiri, Y.: Global sea–air CO$_2$ flux based on climatological surface ocean $p$CO$_2$ and seasonal biological and temperature effects, Deep-Sea Res. Pt. II, 49, 1601–1622, 2002.

Takahashi, T., Sutherland, S. C., Wanninkhof, R., Sweeney, C., Feely, R. A., Chipman, D. W., Hales, B., Friederich, G., Chavez, F., Sabine, C., Watson, A., Bakker, D. C. E., Schuster, U., Metzl, N., Yoshikawa-Inoue, H., Ishii, M., Midorikawa, T., Nojiri, Y., Kortzinger, A., Steinhoff, T., Hoppema, M., Olafsson, J., Arnarson, T. S., Tilbrook, B., Johannessen, T., Olsen, A., Bellerby, R., Wong, C. S., Delille, B., Bates, N. R., and de Baar, H. J. W.: Climatological mean and decadal change in surface ocean $p$CO$_2$, and net sea–air CO$_2$ flux over the global oceans, Deep-Sea Res., 56, 554–577, doi:10.1016/J.Dsr2.2008.12.009, 2009.

Takahashi, T., Sweeney, C., Hales, B., Chipman, D. W., Newberger, T., Goddard, J. G., Iannuzzi, R. A., and Sutherland, S. C.: The changing carbon cycle in the Southern Ocean, Oceanography, 25, 26–37, 2012.

Taylor, K. E.: Summarizing multiple aspects of model performance in a single diagram., J. Geophys. Res.-Atmos., 106, 7183–7192, 2001.

Thomalla, S. J., Fauchereau, N., Swart, S., and Monteiro, P. M. S.: Regional scale characteristics of the seasonal cycle of chlorophyll in the Southern Ocean, Biogeosciences, 8, 2849–2866, doi:10.5194/bg-8-2849-2011, 2011.

Thomas, H., Prowe, A. E. F., Lima, I. D., Doney, S. C., Wanninkhof, R., Greatbatch, R. J., Schuster, U., and Corbiere, A.: Changes in the North Atlantic Oscillation influence CO$_2$ uptake in the North Atlantic over the past 2 decades, Global Biogeochem. Cy., 22, GB4027, doi:10.1029/2007gb003167, 2008.

Thompson, D. W. J. and Solomon, S.: Interpretation of Recent Southern Hemisphere Climate Change, Science, 296, 895–899. doi:10.1126/science.1069270, 2002.

Wanninkhof, R. : Relationship between wind speed and gas exchange over the ocean, J. Geophys. Res., 97, 7373–7382, doi:10.1029/92JC00188, 1992.

Wanninkhof, R., Park, G.-H., Takahashi, T., Sweeney, C., Feely, R., Nojiri, Y., Gruber, N., Doney, S. C., McKinley, G. A., Lenton, A., Le Quéré, C., Heinze, C., Schwinger, J., Graven, H., and Khatiwala, S.: Global ocean carbon uptake: magnitude, variability and trends, Biogeosciences, 10, 1983–2000, doi:10.5194/bg-10-1983-2013, 2013.